JACS Au
AN OPEN ACCESS JOURNAL OF THE AMERICAN CHEMICAL SOCIETY

Editors' Choice
Open Access

pubs.acs.org/jacsau
Perspective

Dynamic Evolution of Catalyst Structure for Tuned Catalytic Performance in CO_2 Hydrogenation

Xiangze Du, Yamei Fan, Jun Fan, Xiaoyue Wang, Rongtan Li, Wenjing Bao, and Qiang Fu*

Cite This: https://doi.org/10.1021/jacsau.5c01671
Read Online

ABSTRACT: Dynamic structural evolution of a catalyst often occurs during the CO_2 hydrogenation reaction, and such controllable evolutions can be utilized to optimize catalyst structure and improve catalytic performance. In this Perspective, we highlight evolution processes caused by the coexistence of both oxidizing and reducing atmospheres in this reaction, including alloying/dealloying from metal diffusion, oxide/metal interface formation driven by strong metal−support interactions, oxide/oxide interface formation driven by strong oxide−support interactions, redispersion of metal and oxide, and chemical phase transformations. These dynamic structural evolutions are determined by the redox potential of the reaction atmosphere and the confinement effect of the microenvironment. Controlling specific dynamic evolution can achieve modulated catalytic performance including improved activity, altered selectivity, and enhanced stability, which provides insight for rational design of catalysts in C1 conversion. To conclude, personal perspectives are provided on constructing active sites with high activity and stability for the target products by using a reaction-induced *in situ* synthesis method.

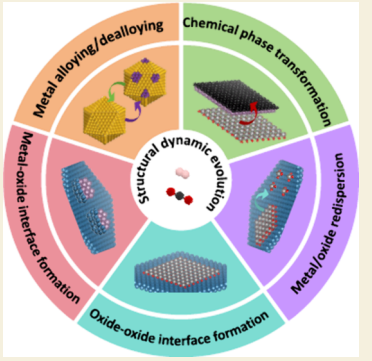

KEYWORDS: *Dynamic evolution, (de)alloying, oxide/metal interface, oxide/oxide interface, redispersion, phase transformation, CO_2 hydrogenation*

1. INTRODUCTION

In heterogeneous catalysis, solid catalysts often experience dynamic structural evolution due to their interactions with gas or liquid phase reaction molecules. These processes can be understood as restructuring of surface atoms or bulk structures of the catalyst in the reaction microenvironment.[1−3] This structural evolution is often a prerequisite for catalyst activation, transforming the as-synthesized material into its active state. However, an uncontrollable change may also drive the catalyst away from this optimized state, leading to deactivation. Therefore, a central challenge lies in understanding and controlling these dynamics to stabilize the active (often metastable) state while mitigating pathways toward irreversible deactivation. Nowadays, the analysis and understanding of active sites at an atomic or molecular level have become facile via surface/interface characterization techniques, which can aid in optimizing and designing catalyst structures. Furthermore, reaction-induced *in situ* or *operando* structural evolutions of the catalyst show a straightforward and effective way to tune catalytic performance, including enhancing catalytic activity, altering selectivity, and improving catalyst stability.[4−6]

There are various structural changes of catalysts under reaction conditions, including oxidation/reduction,[7,8] dispersion/sintering,[9,10] encapsulation/de-encapsulation,[11] segregation/diffusion,[12] dissolution/precipitation,[13] and nitridation/carburization,[14,15] which influence particle size, morphology, composition, and surface/interface or bulk structure of the catalyst. A new equilibrium state is eventually reached, which exhibits a new catalytic performance. These changes are influenced by many factors such as reaction temperature, pressure, external field, atmosphere composition, and interaction with the neighboring microenvironment. It is thus important to elucidate the influencing factors of the structural dynamic evolution during the reaction, which can help specifically inhibit unfavorable structural evolution and thus enhance performance.

Conversion of CO_2 into high-value products by using green hydrogen not only helps to reduce greenhouse gas emissions but also optimizes the energy structure by decreasing excessive dependence on fossil fuels and increasing storage of renewable energy.[16] The reaction products mainly include CO, methanol, CH_4, and C_{2+}. Among them, methanol and CO constitute the two main value chains for converting CO_2 into useful products by various reactions, such as methanol to olefins and Fischer−Tropsch synthesis. The investigation of structural evolution in

Received: December 10, 2025
Revised: February 4, 2026
Accepted: February 5, 2026

https://doi.org/10.1021/jacsau.5c01671
JACS Au XXXX, XXX, XXX−XXX

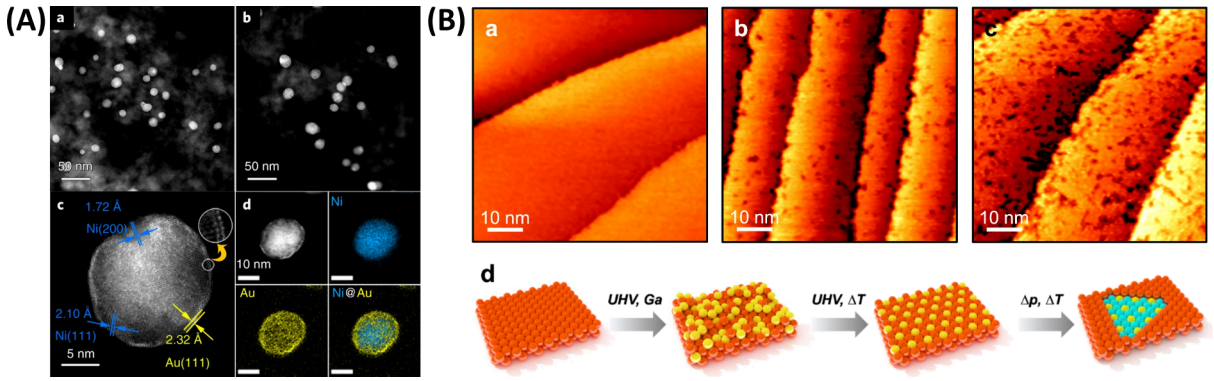

Figure 1. (A) High-angle annular dark-field (HAADF) images of the AuNi/SiO_2 catalyst (a) before and (b) after reaction, (c) atomically resolved HAADF image of one Ni@Au core−shell NP after the reaction, and (d) energy dispersion spectroscopy element mappings. Reproduced with permission from ref 17. (B) Near ambient pressure scanning tunneling microscopy (NAP-STM) images of 2D GaO_x on Ga-Cu obtained in a $CO_2 + H_2$ (1:3) reaction atmosphere: (a) 10^{-2} mbar at 300 K (0.5 V, 0.3 nA), (b) 1 mbar at 300 K (0.4 V, 1 nA), and (c) 1 mbar at 373 K (0.3 V, 1 nA), and (d) structural evolution of the Cu(111) surface at different atmospheres. Adapted with permission from ref 20.

CO_2 hydrogenation is of significance for CO_2 conversion, which can provide insights into other important reactions, such as the water−gas shift reaction, methanol reforming reaction, syngas conversion, and dry reforming of methane. However, probing such structural dynamics under the CO_2 hydrogenation conditions remains highly challenging. On one hand, the CO_2 hydrogenation reaction contains both oxidizing atmospheres (e.g., CO_2 and H_2O) and reducing atmospheres (e.g., H_2, CO, and CH_4). The coexistence of these complex atmospheres often leads to various alterations in the catalyst structure under the reaction conditions. On the other hand, the actual active structure may be observed only through *in situ* or *operando* techniques.

In this Perspective, we provide a comprehensive understanding of structural dynamic evolution during CO_2 hydrogenation reactions and consider how to utilize controllable structural evolution to modulate the catalytic performance of CO_2 hydrogenation. We specifically discuss metal alloying/dealloying from reaction-induced metal diffusion, oxide/metal interface formation due to strong metal−support interaction (SMSI), oxide/oxide interface formation due to strong oxide−support interaction (SOSI), redispersion of metal and oxide, and reaction-driven chemical phase transformations. The increase in the amount of interface active sites, coordinatively unsaturated metal sites, or oxygen vacancies and the formation of new active phases are discussed, which enhance CO_2 conversion, alter selectivity, and improve the stability of the catalyst. Finally, the Perspective looks ahead to future research for designing and guiding *in situ* generation of highly active and stable structures using dynamic structural evolution combined with multiscale simulations and theoretical calculations.

2. REACTION-INDUCED STRUCTURAL EVOLUTION OF THE CATALYST

Both oxidizing gases (CO_2 and H_2O) and reducing gases (H_2, CO, etc.) are present during CO_2 hydrogenation. The catalyst structure is determined by its intrinsic properties and multiple atmospheres and is prone to reach a stable state in such atmospheres. Structural evolutions such as sintering, aggregation, encapsulation, or reduction/oxidation are often linked to catalyst deactivation. However, as illustrated later in this Perspective, their effects are not universally detrimental. The same type of structural change (e.g., oxidation) can be either deactivating or activating, depending critically on the initial catalyst state, the extent of transformation, and the targeted reaction pathway. Therefore, the central objective is to precisely understand and control them to steer the catalyst toward and maintain its optimal active state. The redox potential and confinement effect of microenvironment during the reaction are key factors in surface reconstruction and chemical phase transformation. It is crucial to achieve controlled structural evolution through the redox process and confinement, thereby optimizing catalytic performance.

2.1. Alloying/Dealloying

Surface atoms of metal catalysts can migrate under thermal effects and gas molecule adsorption/desorption effects, leading to surface reconstruction during the reaction. For example, bimetallic catalysts may exhibit structural changes such as alloying or dealloying. Ni atoms in the cores of Ni@Au nanoparticles supported on SiO_2 can gradually segregate to the surface and then form NiAu alloy under CO_2 hydrogenation reaction conditions.[17] The catalyst reforms a Ni@Au core−shell structure after stopping and cooling the reaction, as shown in Figure 1A. Theoretical calculations and *in situ* Fourier-transform infrared spectroscopy (FT-IR) results indicate that *in situ*-generated CO interacts with Ni to form the NiAu surface, generating positive feedback and enhancing the CO selectivity to over 95%. The formation of these alloy nanoparticles is crucial in constructing an active interfacial alloy and plays a significant role in the production of reaction intermediates or products. InO_x can migrate from SiO_2 support to PdCu nanoparticles in H_2 at 300 °C, accompanied by surface segregation of Pd and formation of PdIn alloy.[18] Then *in situ*-formed InO_x/PdIn and InO_x/Cu dual interfaces in CO_2 hydrogenation improve the production rate and selectivity of methanol (5.4 $g_{MeOH} \cdot g_{metal}^{-1} \cdot h^{-1}$). In_2O_3 will also be partially reduced to InO_x and migrate to the surface of Pd.[19] The formed $InPd_x$ alloy particles are partially wrapped by the InO_x layer, enhancing methanol yield.

Dealloying is another important dynamic phenomenon for bimetallic catalysts in CO_2 hydrogenation. The structure of PtMn/SiO_2 catalysts can be modified using reverse water−gas shift (RWGS) reaction atmospheres,[21] where some Mn atoms are removed from the surface during the treatment, resulting in a Pt-rich surface structure. A Pt-rich surface on PtCo nanoparticles during CO_2 hydrogenation can be observed using ambient pressure X-ray photoelectron spectroscopy (AP-XPS) with different incident photon energies.[22] Additionally, two-

https://doi.org/10.1021/jacsau.5c01671
JACS Au XXXX, XXX, XXX−XXX

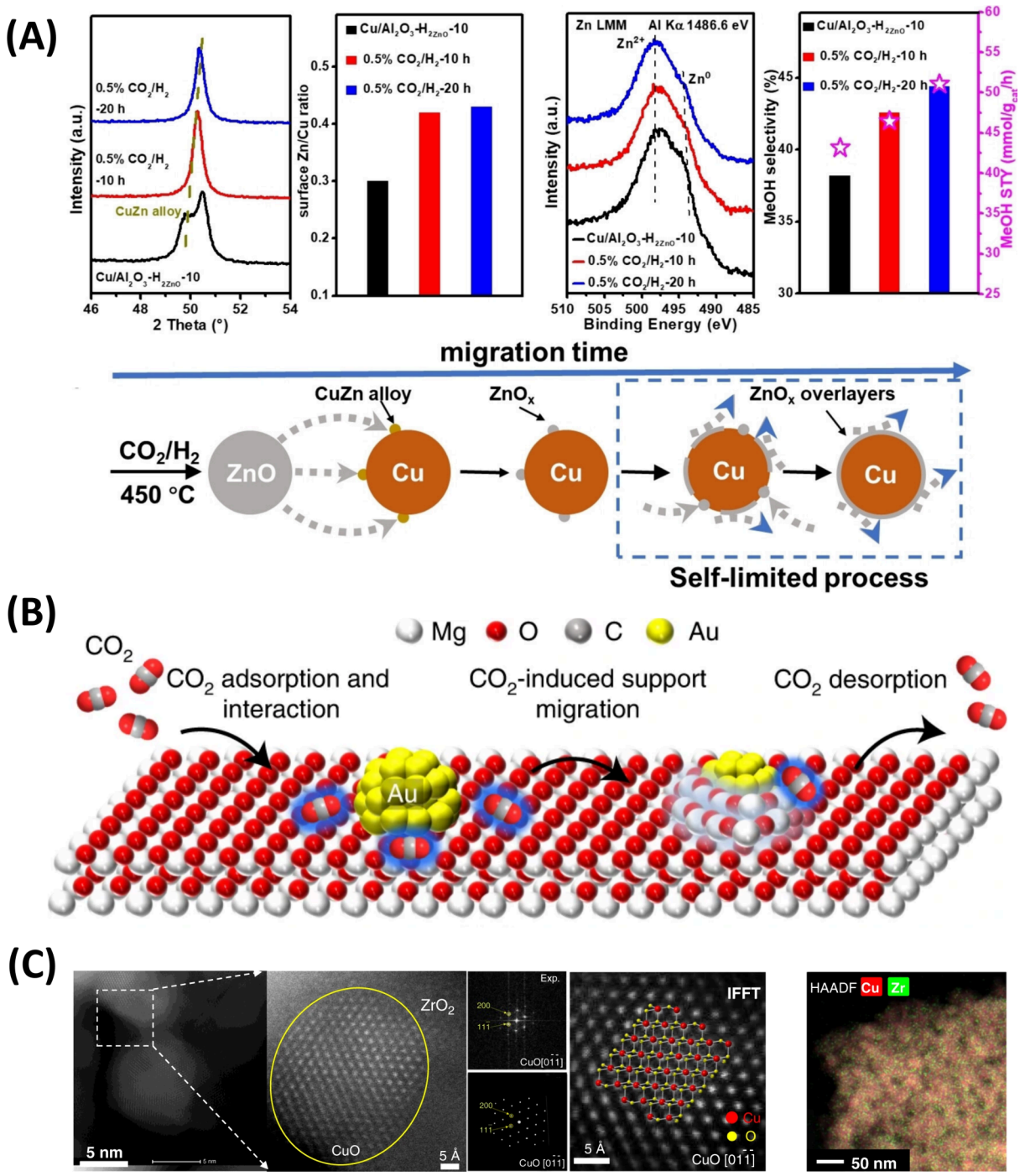

Figure 2. (A) Structure characterization and schematic illustration of the formation of a self-limited Cu@ZnO_x structure under CO_2/H_2. Reproduced with permission from ref 31. (B) Schematic illustration of CO_2-induced activation of MgO to construct SMSI on the Au/MgO catalyst. Reproduced with permission from ref 32. (C) High-resolution HAADF−scanning transmission electron microscopy (STEM) images/fast Fourier transform patterns with simulated results and the energy dispersive spectrometry elemental mapping of the ZrO_2/Cu-0.1 catalyst. Reproduced with permission from ref 33.

dimensional (2D) GaO_x domains with approximately a few atomic layers form on GaCu alloy surface in CO_2 hydrogenation (Figure 1B),[20] which exhibit distinct morphology and properties from bulk Ga_2O_3. These results demonstrate a method for optimizing bimetallic catalyst structure and enhancing the catalytic activity in CO_2 hydrogenation.

Gas-phase chemical potential is the dominant thermodynamic driving force for alloying/dealloying. High reduction potential (high H_2/CO partial pressure) promotes the reduction of highly reducible metal oxides (such as In and Ni oxides) and their integration into alloys. High oxidation potential (high CO_2/H_2O partial pressure) oxidizes metal components (such as Mn and Ga), leading to dealloying. The oxygen affinity of metals also plays a significant role in alloying/dealloying.[23] Metals with different oxygen affinities will selectively migrate (such as Mn and Pt) in a CO_2 hydrogenation atmosphere. Mobility of surface species influences alloying/dealloying processes. Metals with high mobility (such as Au, Cu, and Pd) are more prone to

https://doi.org/10.1021/jacsau.5c01671
JACS Au XXXX, XXX, XXX−XXX

surface segregation for alloying/dealloying. Meanwhile, strongly adsorbed species (such as CO) can significantly change the surface migration barrier of metal atoms and induce their alloying.

Generally, the alloying/dealloying process is reversible and controllable when the reaction atmosphere changes during the oxidation/reduction cycle. For example, switching the feed gas can achieve a controllable alloying/dealloying process by a H_2-rich atmosphere (alloying) or a CO_2-rich atmosphere (dealloying). Moreover, metal alloying/dealloying processes are also accompanied by the formation of oxide/metal and oxide/oxide interfaces during CO_2 hydrogenation, which will be discussed in detail in Sections 2.2 and 2.3 below. These processes provide various active sites for CO, CH_4, and methanol production, making it possible to tune the product selectivity in CO_2 hydrogenation.

2.2. Oxide/Metal Interface Formation

The strong metal−support interaction (SMSI) is one of the typical phenomena in the structural evolution of supported metal catalysts, which creates oxide/metal interface sites. There are many recent reports summarizing the types, mechanisms, and applications of SMSI.[24−28] This interaction mainly involves the migration of reducible oxide supports (such as CeO_2, TiO_2, and Nb_2O_5) onto the metal surface after high-temperature H_2 treatment and the formation of an encapsulating structure. The intrinsic properties of metal and support influence the SMSI processes. The electronic properties of metals can affect metal−support affinity. For example, electron-rich metals may have stronger interactions with electron-deficient suboxide supports. The crystal structure, defect concentration, and crystal facets of the support greatly affect the migration ability of surface species. The gas-phase chemical potential is a crucial factor in inducing SMSI. A high reduction potential facilitates the generation of SMSI, while a high oxidation potential eliminates SMSI. The driving force for the migration of low-valence oxide layers is mainly the reduction of surface energy. The formation of encapsulation structures often alters the adsorption/desorption processes of reaction molecules. This phenomenon allows for effective regulation of the selectivity of target products while maintaining the stability of the catalyst.

Our previous research found that CO_2/H_2 reaction atmosphere could induce SMSI between Ru and MoO_3.[29] MoO_{3-x} defect layer formed by the reduction of MoO_3 migrates onto the Ru surface, producing an encapsulated Ru@MoO_{3-x} structure. This structural evolution changes the selectivity from CH_4 formed on surface Ru sites to CO produced by defective MoO_{3-x} overlayers. A similar result is reported on Ru/anatase-TiO_2 catalyst.[30] The formation of the encapsulated structure of Ru@TiO_x changes the surface reaction intermediate from formate to carboxy species during CO_2 hydrogenation, which alters the selectivity from CH_4 to CO.

The essence of SMSI is the migration of oxides to the metal surface under atmospheric treatment. It shows a promising way to construct highly active catalysts. Researchers have recently loaded oxides onto metal surfaces, i.e., oxide/metal inverse catalysts, to form more active oxide/metal interfacial sites, significantly enhancing catalytic performance. We found that ZnO can undergo surface evaporation and gas-phase migration in H_2, which can be captured by Cu nanoparticles to form surface CuZn alloys.[31] CO_2/H_2 atmosphere can induce the oxidation segregation and surface enrichment of Zn species in the CuZn alloy, subsequently generating ZnO_x on the CuZn alloy surface, as shown in Figure 2A. The ZnO_x encapsulation layer formed in a 0.5% CO_2/H_2 atmosphere is self-limiting, preventing excessive deposition and aggregation of ZnO_x. The formation of the ZnO_x encapsulation layer significantly enhances the methanol yield of the Cu/Al_2O_3 catalyst in CO_2 hydrogenation.

Utilizing CO_2 hydrogenation reaction intermediates to promote SMSI formation is one of the methods for constructing encapsulated active structures. Recently, an adsorbate (HCO_x)-mediated SMSI (A-SMSI) mechanism was proposed, where the encapsulation layer is permeable to reactants and not easily oxidized.[34] A-SMSI depends on a CO_2-rich ($20CO_2$:$2H_2$) atmosphere, which, however, disappears gradually in pure H_2. CO_2 hydrogenation reaction atmospheres with a CO_2/H_2 ratio from 1:1 to 4:1 usually render the A-SMSI encapsulation layer unstable. The initial oxygen vacancy concentration of oxide supports can regulate the formation conditions of A-SMSI.[35] After increasing the initial oxygen vacancy concentration of TiO_2, the formed A-SMSI state remains stable under the reaction conditions ($1CO_2$:$1H_2$).

Typically, the reduction of metal oxide supports by H_2 is the key to constructing SMSI. However, Wang et al. utilized Le Chatelier's principle to achieve SMSI on Au nanoparticles supported on nonreducible oxides (MgO) by CO_2 (Figure 2B),[32] expanding the understanding and application scope of SMSI. Acidic CO_2 initially reacts with the basic support to form carbonates, such as $MgCO_3$, which migrates and encapsulates Au and then decomposes at suitable temperatures to form more MgO/Au interfaces. Since the melting point of carbonates is generally lower than that of the corresponding oxides, utilizing this property to activate oxides like MgO, ZnO, and CaO is a strategy worth considering for constructing SMSI. In addition, SMSI is also found on the $BaCO_3$-supported Ni catalyst.[36] $BaCO_3$ is prone to decompose by Ni nanoparticles in H_2 but regenerate in CO_2/H_2 atmosphere. This sustainable decomposition-regeneration process leads to CO_2 enrichment at the Ni-$BaCO_3$ site, which enhances CO_2 adsorption and activation to promote the CO_2 methanation reaction.

The formation of SMSI brings about abundant oxide/metal interfacial sites, thereby enhancing the CO_2 conversion or changing the selectivity. Nowadays, more and more oxide/metal inverse catalysts have been designed and used for CO_2 hydrogenation to methanol, including ZnO_x/Cu,[37−39] ZrO_x/Cu,[33,40−42] $ZnZrO_x$/Cu,[43,44] CeO_x/Cu,[45] ZrO_x/Ni,[46] and FeO_x/Rh-Fe.[47] The partially reduced amorphous ZrO_2 (1−2 nm) can anchor onto the metal Cu surface in nanoislands on inverse ZrO_2/Cu catalyst (Figure 2C), exhibiting high CO_2 activation ability.[33] The methanol formation rate is three times that of traditional Cu/ZrO_2 catalysts. Meanwhile, interfacial ZrO_x stabilizes the Cu nanoparticles and improves the catalyst stability. Additionally, $CeAlO_x$/Ni catalysts used for CO_2 methanation[48] and TiO_2/Cu catalysts employed in the RWGS reactions were also reported.[49]

2.3. Oxide/Oxide Interface Formation

Oxide catalysts play important roles in many catalytic reactions, such as alkane deoxygenation,[50,51] syngas conversion,[52,53] hydrogenation reaction,[54,55] oxygen evolution reaction,[56,57] and hydrogen evolution reaction.[58,59] Bond and Wachs et al. discovered that the dispersion degree and catalytic performance of oxides are closely related to the supports.[60,61] For example, vanadium oxide tends to form highly dispersed monolayers or clusters on TiO_2, while it more readily forms three-dimensional

https://doi.org/10.1021/jacsau.5c01671
JACS Au XXXX, XXX, XXX−XXX

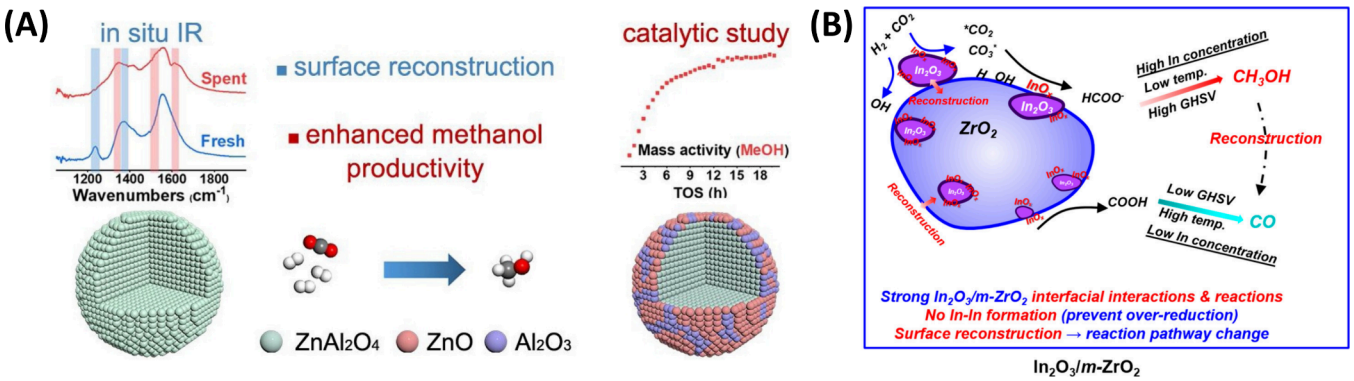

Figure 3. (A) Scheme of surface reconstruction of $ZnAl_2O_4$ to form amorphous ZnO and enhance the methanol yield. Reproduced with permission from ref 66. (B) Selectivity modulation in CO_2 hydrogenation by reversible InO_x entering and exiting the ZrO_2 subsurface. Reproduced with permission from ref 68. Copyright 2022 American Chemical Society.

V_2O_5 crystallites on SiO_2.[61] This structural difference and the resulting significant changes in catalytic performance were attributed to the strong interaction between the surface oxide and the support. Then strong oxide-support interaction (SOSI) has attracted much attention and plays a significant role in oxide catalysis. Recently, we reported the local interfacial confinement effect between Co oxide and ZnO support in Co_3O_4/ZnO prepared by an impregnation method.[62] A metastable CoO_x state is maintained in the CO_2 hydrogenation reaction and produces 93% CO selectivity. In contrast, the reduction of Co_3O_4 to Co^0 is significantly promoted in a physically mixed Co_3O_4 and ZnO powder (Co_3O_4-ZnO), which thus shows high selectivity toward CH_4 (92%). It reveals a distinct SOSI mode, i.e., local interfacial confinement and remote spillover effects at the oxide−oxide interfaces determined by the distance of oxides, which allow the modulation of product selectivity in CO_2 hydrogenation. In addition, the interfacial oxygen species (Mn-O-Ce) formed by SOSI can efficiently activate propane.[63] The coordinatively unsaturated manganese sites generated on the catalyst surface can effectively adsorb and stabilize propylene, significantly improving propylene selectivity compared to MnO_2.

Similar to SMSI, SOSI is a complex interface engineering process that is thermodynamically driven (reducing interface and surface energy), kinetically controlled (temperature and mobility), triggered by external chemical potential (oxidation potential), and enhanced by electronic coupling between the oxide and support. The key to ensuring reversibility and stability lies in preventing the support or oxide from being over-reduced. There is an SOSI state to facilitate oxide/oxide interface formation, which plays a significant role in catalytic reactions. For example, CoO_x-InO_x interfacial sites can be formed in physically mixed Co_3O_4-In_2O_3, Co_3O_4/In_2O_3 and Co-InO_x catalysts during CO_2 hydrogenation, enhancing methanol selectivity.[64] Defects at the Fe_2O_3−Al_2O_3 interface were created between highly dispersed Fe_xO_y particles and γ-Al_2O_3 support due to SOSI.[65] The defects result in more active oxygen species at the interface to form HCOO*, CH_3O*, and HCO_3* intermediates, which enhance CH_3OH synthesis from the CO_2/H_2 plasma reaction.

Oxide separation or recombination can form some special interfacial structures to enhance the CO_2 conversion. For example, the reconstruction of ZnO significantly improves the catalytic activity in Zn-based spinel or mixed oxides in CO_2 hydrogenation. The surface reconstruction of $ZnAl_2O_4$ to form amorphous ZnO overlayers (Figure 3A)[66] and the formation of ZnO_x clusters on ZnO/ZrO_2[67] promote H_2 activation and accelerate the methanol formation rate. The formation of oxide solid solutions or spinel structures in composite oxides during reactions is another important approach to enhance the oxygen vacancy concentration and improve the CO_2 adsorption and activation. In addition, the formed InO_x in reaction can semireversibly enter the subsurface of monoclinic ZrO_2 (*m*-ZrO_2), and the variation in InO_x concentration due to reconstruction under different reaction conditions may be a key factor influencing the catalytic activity, as shown in Figure 3B.[68] With an increasing reaction temperature, the surface concentration of InO_x decreases, leading to an enhancement of CO selectivity and a significant reduction in methanol selectivity.

Nowadays, it has become increasingly critical to design catalyst structures in a targeted manner and enhance CO_2 hydrogenation performance using SOSI. The chemical looping CO_2 conversion can be enhanced by utilizing SOSI between Fe_2O_3 and ZrO_2.[69] The electronic oxide-support interaction between Fe_2O_3 and *m*-ZrO_2 is stronger than that of tetrahedral ZrO_2 (*t*-ZrO_2), which facilitates the formation of more oxygen vacancies at the Fe_2O_3−ZrO_2 interface to promote CO_2 activation and H_2 adsorption, enhancing CO_2 conversion to CO. CO_2/H_2 reaction atmosphere can facilitate the reduction of In_2O_3 by supported Ru clusters to form In_2O_{3-x} aggregates and RuO_x−In_2O_{3-x} interfacial sites.[70] The product selectivity shifts from CH_4 to methanol generated by the formed RuO_x−In_2O_{3-x} interface.

2.4. Redispersion of Metal and Oxide

The degree of dispersion of the nanostructures on the support influences the activity and stability of the catalyst. In most cases, increasing the metal dispersion contributes to high catalytic performance. The thermodynamic driving force for redispersion is to reduce the total energy of the system. When the interfacial energy of the metal/oxide−support is lower than the surface energy of the support, the metal or oxide tends to wet on the support surface to achieve redispersion. Meanwhile, the redox flexibility of the metal or oxide, gas-phase chemical potential, and mobility of the surface species determine the final redispersion degree. An obvious characteristic of redispersion is the reduction in the size of nanoparticles to form clusters or even single atoms, which affects the geometric and electronic structure of catalytic sites and, thereby, governs product selectivity.

https://doi.org/10.1021/jacsau.5c01671
JACS Au XXXX, XXX, XXX−XXX

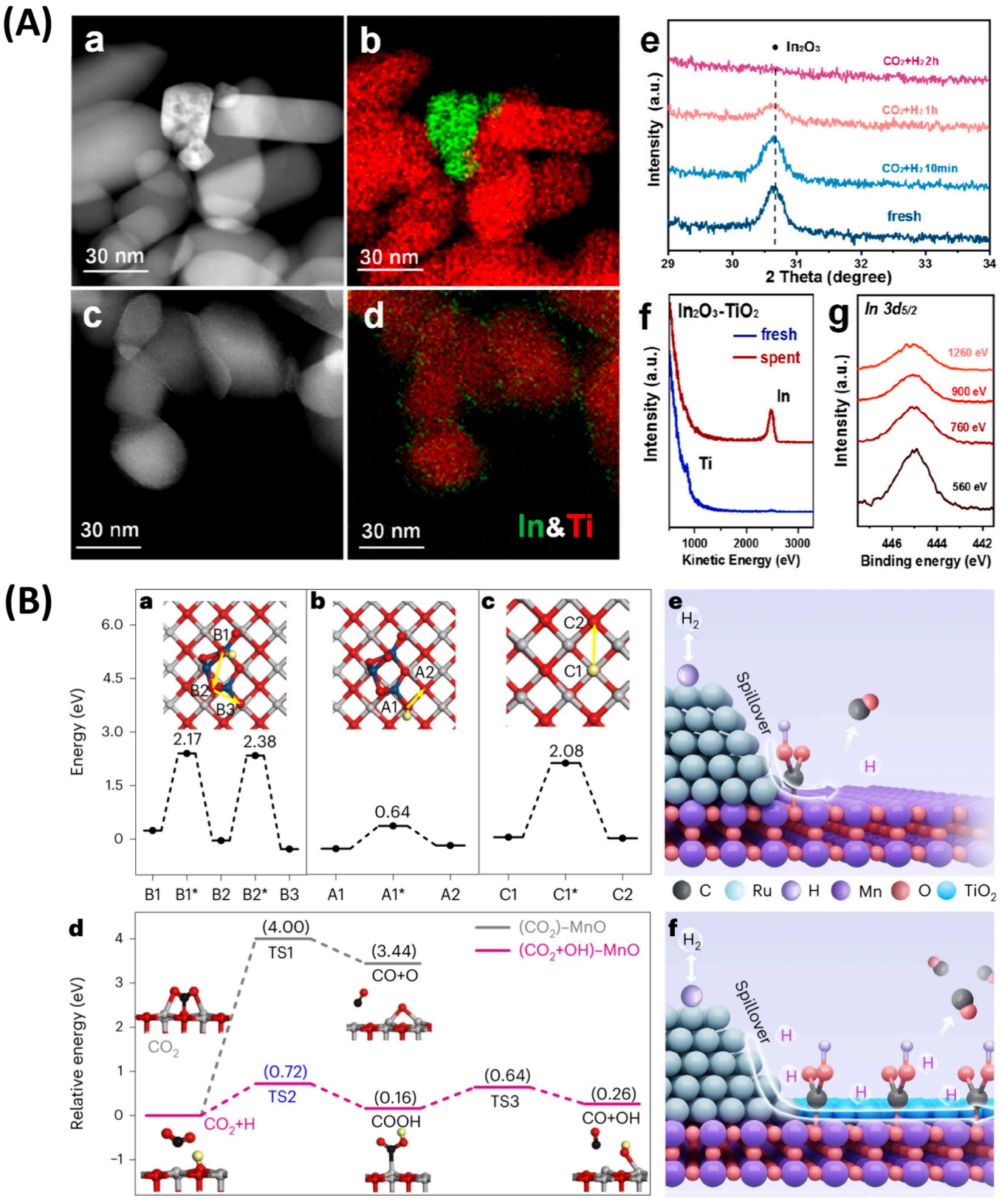

Figure 4. (A) Structural evolution of the In_2O_3−TiO_2 catalyst during the RWGS reaction: HAADF-STEM and energy-dispersive X-ray spectroscopy mapping images of (a-b) fresh and (c-d) spent In_2O_3−TiO_2, (e) *in situ* X-ray diffraction (XRD) patterns of In_2O_3−TiO_2 during the RWGS reaction, (f) HS-LEIS spectra of fresh and spent In_2O_3−TiO_2 samples, and (g) *in situ* XPS In $3d_{5/2}$ spectra acquired with different X-ray energies. Reproduced with permission from ref 80. Copyright 2024 American Chemical Society. (B) Hydrogen migration energy barriers over (a) TiO_2 overlayer, (b) TiO_2/MnO interface, and (c) MnO surface, (d) energy profiles of the RWGS reaction on the MnO (100) surface with and without hydrogen species, and reaction pathway schemes for (e) Ru/MnO and (f) the Ru/Ti/Mn ternary interface. Reproduced with permission from ref 82.

https://doi.org/10.1021/jacsau.5c01671
JACS Au XXXX, XXX, XXX−XXX

CO_2 can react with carbon-based supports to form carbonyl and carboxylate groups,[71] which can serve as anchoring sites for metal atoms/clusters.[72] A redispersion of the detached Cu atoms/clusters was reported on a carbon-supported Cu catalyst in CO_2 hydrogenation.[73] The redispersion of Ni nanoparticles can decrease the size from 12.9 to 3.1 nm, which reduces the rate of formate intermediate formation and promotes CO generation.[74] The redispersion of Re clusters brought about the formation of smaller clusters and single-atom Re in CO_2 hydrogenation,[75] increasing $Re^{\delta+}$ species and, correspondingly, a decrease of the fraction of Re^0 species. Nevertheless, a portion of Re^0 is still retained in the (sub)nanoclusters. These two sites are responsible for activating CO_2 and the formation of Re-H, which is able to form active formate and undergo further hydrogenation to methanol.

The products in CO_2 hydrogenation, such as CO, H_2O, and methanol, will also influence the metal redispersion. CO can induce Rh particles to form atomically dispersed Rh species on Y zeolite, forming the main CH_4 product.[76] The formation of the metal−CO complex is usually considered the key intermediate in the redispersion of the metal catalyst. Our recent work found that H_2O also facilitates the redispersion of Cu from nanoparticles to single atoms.[77] H_2O induces the formation of hydroxylated Cu species and surface OH groups, which help to pull the mobile Cu species and enhance the Cu redispersion. The formation of hydroxylated metal species and hydroxylated support provides another route to disperse metal catalysts. Additionally, methanol can also promote the redispersion of metallic Cu. Methanol can trigger Cu−Cu bond cleavage and facilitate the formation of $(CHO)Cu_1$* intermediate.[78] Silanol nests trap the migratable Cu sites to form small nanoparticles and achieve redispersion on dealuminated Beta zeolite. Although these processes were observed in other hydrogenation reactions, the method remains valuable for catalyst structure optimization and design, given that these molecules can be produced in CO_2 hydrogenation.

Recently, the redispersion of oxide has attracted widespread attention in the field of heterogeneous catalysis. This process is also relevant with the oxide/oxide interface formation by SOSI. For example, In_2O_3 can migrate and disperse on the surface of ZrO_2 by SOSI in CO_2 hydrogenation, promoting electron transfer and effectively increasing the methanol yield.[79] Indeed, SOSI helps oxide to disperse onto the support effectively. In most cases, oxide nanolayers are formed after redispersion due to SOSI. We have found the dispersion phenomenon on In_2O_3−TiO_2 catalyst prepared by physically mixing In_2O_3 and TiO_2.[80] In_2O_3 is reduced to metallic In by H_2 and then anchored by hydroxyl groups on the TiO_2 surface to form In−O−Ti bonds, achieving monolayer dispersion in the CO_2 hydrogenation reaction, as shown in Figure 4A. The interface confinement effect between the In_2O_3 nanolayer and TiO_2 promotes the partial reduction of the In_2O_3 thin layer and formation of rich oxygen vacancies. Meanwhile, it simultaneously inhibits the over-reduction of In_2O_3 to metallic In. The confined InO_x nanolayer is kept in a metastable state during the reaction, thus improving both catalytic activity and stability. This interface confinement effect can also be extended to multiple In_2O_3−oxide interfaces, exhibiting good universality.[80] Additionally, the partially reduced InO_x species exhibit periodic aggregation−redispersion behavior on m-ZrO_2.[81] The authors explain that the chemical potential driven by the H_2 atmosphere or electron beam leads to InO_x aggregation, while the increased strain between the growing InO_x and the interfacial structures on m-ZrO_2 destabilizes the aggregation and facilitates its redispersion. This dynamic process helps maintain a highly active phase dispersion, thereby improving the efficiency of methanol production.

CoO_x nanoparticles (in the largest dimension <2.5 nm) supported on CeO_2 can transform from a pyramidal three-dimensional form to a monolayer structure when H_2 flow is switched to a CO_2/H_2 flow.[83] This process is reversible, and the monatomic layer results in ∼30% CH_4 selectivity. In addition, CO_2 hydrogenation reaction can selectively induce the spontaneous dispersion of TiO_2 onto the surface of MnO, rather than migrating to Ru surface to form an encapsulating structure, as shown in Figure 4B.[82] The TiO_2/MnO interface acts as an efficient hydrogen transfer channel, increasing the concentration of active H species on the MnO surface. Therefore, it promotes the entire hydrogenation process and significantly enhances the RWGS activity of the Ru/(TiO_x)-MnO catalyst.

ZnO on the Cu-Zn-Zr catalyst can undergo redistribution under CO_2 hydrogenation conditions, forming atomically dispersed Zn species on ZrO_2 surface.[84] The dispersed Zn species create a highly active interface with Cu, which reduces the energy barrier for H_2 activation and suppresses the decomposition of intermediates into CO. These interfacial sites significantly outperform the catalytic performance of conventional Cu/ZnO interfaces and isolated ZnO sites, effectively improving the methanol selectivity and yield. Zhang et al. also found that ZnO clusters can further disperse on the surface of t-ZrO_2 in CO_2 hydrogenation.[85] The abundant ZnO−ZrO_2 interfacial sites facilitate the generation of HCOO* species, enhancing the yield and selectivity of methanol. The formation of ZnO clusters on the surface of $ZnZrO_x$ can be observed at 250−280 °C in H_2 atmosphere.[86] When the catalyst is treated in a H_2 flow at 400 °C and then switched to a CO_2/H_2 reaction atmosphere at 350 °C, the ZnO_x size (1−10 nm) gradually decreases and forms more ZnO/ZrO_2 interfacial sites for methanol production.

Redispersion of metal generates more metal/oxide interface sites, which can enhance the CO_2 conversion and promote the selectivity of CO, CH_4, and methanol. For the redispersion of oxide, it forms more oxide/oxide interface sites, which favors CO_2 conversion and improves CO and methanol selectivity. Redispersion of metal or oxide provides more sites for H_2 activation and H spillover, as well as CO_2 adsorption and activation, thereby enhancing catalytic activity.

2.5. Chemical Phase Transformations

Phase transition is one of the important structural evolution phenomena during CO_2 hydrogenation. Chemical phase transformations can be divided into two categories based on whether their composition changes. One is the phase transition with unchanged element composition. For example, the hexagonal-phase h-In_2O_3 can first be reduced to low-valence indium and then oxidized by CO_2 into cubic-phase c-In_2O_3.[87] The surface of c-In_2O_3 is easier to form oxygen vacancies and makes it more active in CO_2 hydrogenation. Besides, a 3:1 ratio of Ga_2O_3 to CeO_2 can form $Ga_xCe_yO_z$ solid solutions and more Ga-O-Ce interface sites, which increase oxygen vacancies and thereby enhance RWGS reaction activity.[88] The formation of $ZnFe_2O_4$ in ZnO−Fe_2O_3−K composite catalyst under reaction conditions can improve C_{2-4} olefin selectivity and catalyst stability.[89] For this phase transition, it is typically driven by the temperature, pressure, or chemical potential of the reaction

https://doi.org/10.1021/jacsau.5c01671
JACS Au XXXX, XXX, XXX−XXX

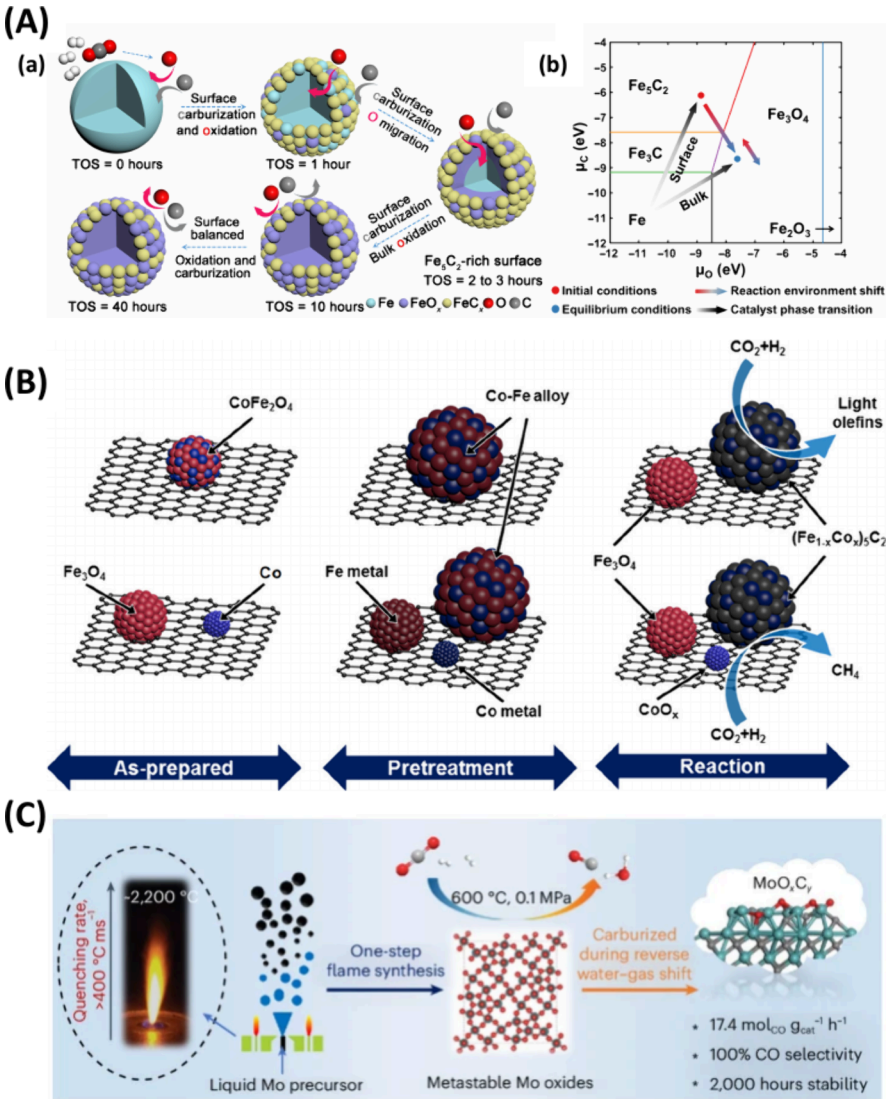

Figure 5. (A) Structural evolution of Fe species during CO_2 hydrogenation: (a) scheme of the evolution process over time and (b) the computed phase diagram of iron, iron carbides, and oxides. Reproduced with permission from ref 97. (B) Schematic illustrations of the phase transformations treated at different atmospheres. Reproduced with permission from ref 101. Copyright 2020 American Chemical Society. (C) Scheme of RWGS reaction-induced cubic α-MoC with surface unsaturated MoO_xC_y formation for high-rate CO production. Reproduced with permission from ref 102.

environment (such as the partial pressure of oxygen) to achieve a more stable thermodynamic state.

Another type is a phase transition with a changed element composition, which is driven by a chemical reaction between the catalyst and atmosphere. The most important process is carburization in this phase transformation. An active ruthenium oxycarbonate (RuO_xC_y) phase can be formed during CO_2 hydrogenation for the selective conversion of CO_2 to CH_4 at lower temperatures.[90,91] The doping of carbon into ruthenium oxide enables the stabilization of Ru cations in a low oxidation state (Ru^{n+}, $0 < n < 4$) and shows an excellent long-term stability. Further studies demonstrate that the CO_2 partial pressure affects the surface coverage of carbon intermediate species, thereby influencing the stabilization of interstitial carbon species in RuO_xC_y.

Transition metals such as Fe and Co can undergo carburization during CO_2 hydrogenation reaction due to the presence of carbon-containing products, significantly enhancing catalytic activity or altering product selectivity.[92−96] Metallic Fe can be transformed into Fe_3C and then Fe_5C_2, and subsequently form a large amount of Fe_3O_4 during CO_2 hydrogenation, as shown in Figure 5A.[97] Finally, a stable Fe_3O_4@(Fe_5C_2 + Fe_3O_4) core−shell structure is formed. The formation of Fe_5C_2 increases the selectivity for the C_{2+} products. Pd single atoms can promote the carburization of FeO_x support, resulting in the highly active Fe_5C_2 phase.[98] The particle size of Pd affected the carburization rate of FeO_x.[99] A large size of Pd nanoparticles (>5 nm) induces the Pd_3Fe formation and alters the reaction route to produce $HCOO^-$, which drives fast surface carburization of Fe and thus enhances the CO formation rate. CO_2 can enhance the migration of K species to the Fe surface by participating in the cyclic conversion process. The formation of Fe_5C_2−K_2CO_3 interface promotes the production of ethylene, propylene, and other linear α-olefins.[100] Additionally, the formation of Fe_5C_2 and the MnO-containing overlayers surrounding the Fe_5C_2 surface hinders methane but favors C_2−C_4 olefins and C_{5+} hydrocarbons formation.[92]

Co-Fe oxide catalysts can form χ-$(Co_xFe_{1-x})_5C_2$ alloy carbides in CO_2 hydrogenation.[103,104] During the reaction, the Fe_xCo_y alloy can be carburized to the pure χ-$(Co_xFe_{1-x})_5C_2$

https://doi.org/10.1021/jacsau.5c01671
JACS Au XXXX, XXX, XXX−XXX

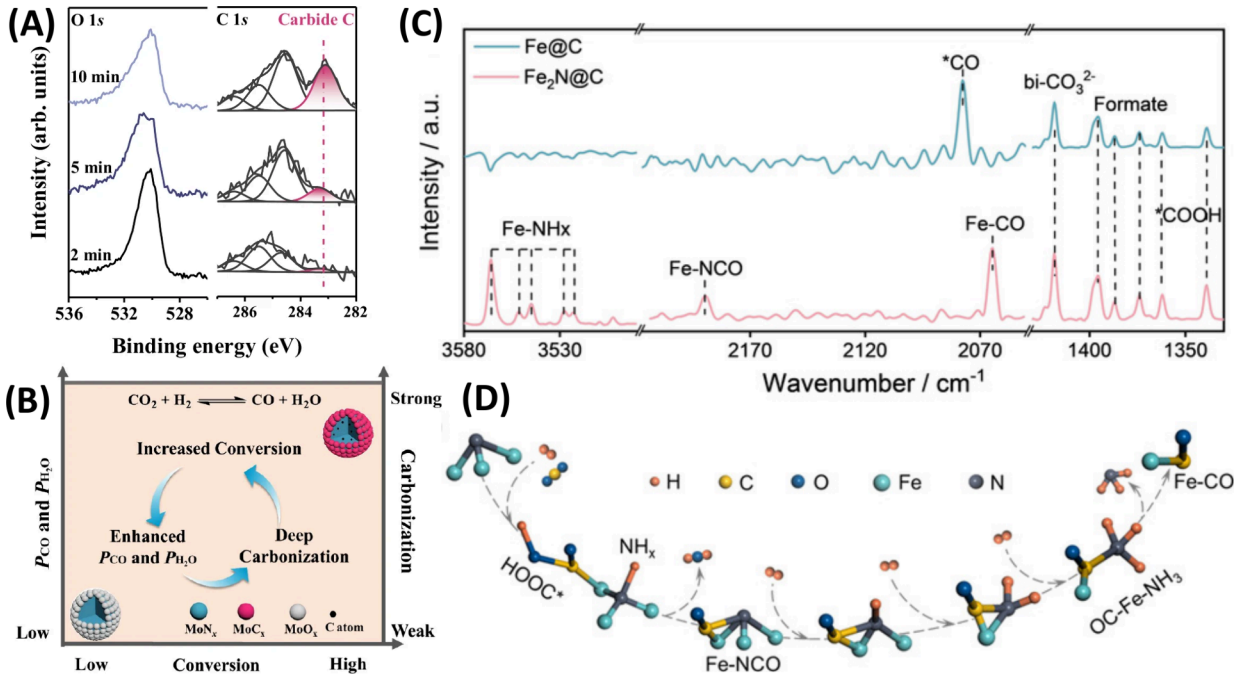

Figure 6. (A) *In situ* XPS C 1*s* spectra of Mo_2N. (B) Scheme of the positive feedback process between RWGS activity and carbonization. Panels A and B reproduced with permission from ref 15. (C) *In situ* DRIFTS of Fe_2N@C in CO_2 hydrogenation. (D) Schematic illustration of the *in situ* carbonization process from Fe_2N to Fe_xC_y. Panels C and D reproduced with permission from ref 111.

phase, which achieves a high olefin space−time yield (1.8 g·g_{cat}^{-1}·h^{-1}). $ZnFe_2O_4$ spinel can gradually transform into a mixture of ZnO and Fe_7C_3 in CO_2 hydrogenation.[105] While Na-containing $ZnFe_2O_4$ can transform into the Fe_5C_2 phase during the reaction. Aromatic products with a selectivity of 75.6% can be obtained when it is coupled with HZSM-5.[106] For Na-containing $CoFe_2O_4$ catalyst, it generates $(Co_xFe_{1-x})_5C_2$ phase under reaction, as shown in Figure 5B.[101] Additionally, Mo modification can inhibit over-carburization of CoFe alloy and promote higher alcohol selectivity,[107] which provides another method to alter selectivity in CO_2 hydrogenation.

The addition of a moderate amount of H_2O and K promoter jointly can promote the formation of surface $CO_2^{\delta-}$ in CO_2 hydrogenation.[108] $CO_2^{\delta-}$ subsequently was dissociated into C* species and facilitates the carburization of CoO into Co_2C. At the same time, the presence of H_2O also inhibits the decomposition of Co_2C into metallic Co. It promotes the selectivity of C_{2+} hydrocarbons from CO_2 hydrogenation on the formed Co_2C efficiently and stably. Ni carbide-like phase can be formed due to the accumulation of carbon species, accompanied by a shift in product selectivity from CH_4 to CO in CO_2 hydrogenation.[109] CH_4 is obtained again after removing carbon species by O_2 treatment, achieving controllable product selectivity for CH_4 and CO.

Recently, we also found that intercalated H could facilitate the reduction of MoO_x and subsequently carburization to MoC_x in CO_2 hydrogenation.[110] Two forms of metallic Mo can be formed in CO_2/H_2 and H_2 atmospheres, which were denoted as Mo1 and Mo2, respectively. Only metallic Mo2 with a lower surface O/Mo ratio favors carburization. The formation of MoC_x facilitates CO_2 adsorption and activation, as well as H_2 activation, significantly enhancing RWGS activity (7544.6 mmol·g_{cat}^{-1}·h^{-1}). Ir/MoO_3 catalyst can also be carburized to form bulk α-MoC and surface MoO_xC_y in the RWGS reaction (Figure 5C), which shows an ultrahigh CO formation rate (17 500 mmol·g_{cat}^{-1}·h^{-1}) at a high space velocity.[102]

In addition to metals or metal oxides, *in situ* carburization has also been observed on nitride catalysts.[15,111,112] We found that the surface structure of molybdenum nitride (MoN_x) catalysts in RWGS highly depends on the partial pressure of products, specifically CO and H_2O.[15] H_2O dominates oxidation of the MoN_x surface to the MoO_x layer at the early stages of the reaction when partial pressure of the product is low. As the reaction proceeds and the product partial pressure increases, the CO in the products dominates the surface carburization to form surface MoC_x. The formed MoC_x promotes the reaction and generates CO with a higher partial pressure, which in turn further stimulates the surface carburization of MoN_x, as shown in Figures 6A and B. This process reveals a positive feedback mechanism between the catalytic activity and structural evolution of the catalyst during the reaction. The carburization of Mo_2N to form α-MoC was also observed by Zhang et al.[113] Both surface and bulk carbon atoms of α-MoC participate in the dynamic carbon flow circulating with gas phase reactants during the RWGS reaction. It highlights the importance of maintaining the stability of metastable α-MoC through such carbon circulation.

The Fe_2N@C catalyst forms iron carbonyl and then converts into iron carbide during CO_2 hydrogenation.[111] As a result, the selectivity of the C_{2+} products is significantly improved. *In situ* diffuse reflectance infrared Fourier transform spectroscopy (DRIFTS) shows that carburization occurs only when CO_2 and H_2 coexist, as illustrated in Figures 6C and D. The phase transition process involves hydrogen dissociation and capture by nitrogen to form NH_x, while CO_2 is activated at the Fe site to form *COOH. Then, NH_x and *COOH undergo dehydration to form a Fe-NCO intermediate, which is further hydrogenated to produce OC-Fe-NH_3 species. After ammonia is removed, the

https://doi.org/10.1021/jacsau.5c01671
JACS Au XXXX, XXX, XXX−XXX

iron carbonyl (Fe-CO) intermediate is obtained and further transformed into an iron carbide.

Chemical phase transformation of the catalyst plays an important role in improving CO_2 conversion and tuning product selectivity. Especially for carburization, the carbides (such as MoC_x and FeC_x) have an outstanding CO_2 activation ability because of their oxygen affinity. Benefiting from the high carbon chemical potential under high CO_2 conversion, metal or nitride can be carburized by the formed product or intermediate (such as CO and $HCOO^-$). MoC_x catalysts exhibit outstanding RWGS activity. FeC_x-based catalysts show promising potential in CO_2 hydrogenation to high-value chemicals, especially light olefins.

3. INFLUENCE OF STRUCTURAL EVOLUTION ON CATALYTIC ACTIVITY, SELECTIVITY, AND STABILITY

Figure 7 summarizes the dynamic structural evolutions and possible product distributions. Among the evolutions, metal

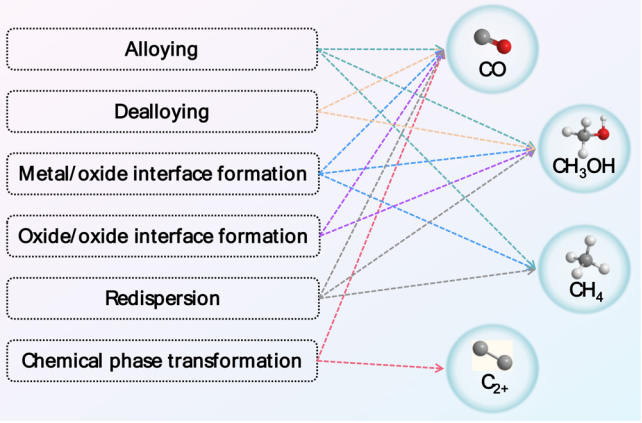

Figure 7. Dynamic structural evolutions and potential selectivity improvement in CO_2 hydrogenation.

alloying/dealloying, metal or oxide redispersion, the formation of oxide/metal and oxide/oxide interfaces, and chemical phase transformation are favorable for the RWGS reaction, resulting in high CO selectivity. RWGS reaction occurs through two main reaction pathways, i.e., the formate route and redox route.[102,114] Due to the altered phase, particle size, morphology, or electronic properties, these newly formed active structures can promote the removal of oxygen through direct dissociation (e.g., MoC_x formation) or decomposition of formate intermediates, thereby facilitating CO generation. In addition, dealloying, redispersion, and the formation of oxide/metal and oxide/oxide interfaces are beneficial for methanol production. CO_2 hydrogenation to methanol mainly occurs through the formate and carboxylate pathways.[115,116] Therefore, the formation of an active structure that can facilitate formate and carboxylate intermediates and further hydrogenation will improve the methanol selectivity. Given this consideration, ZnO_x/Cu and InO_x-based oxide/metal interfaces are widely investigated for methanol production from CO_2 hydrogenation. As for the formation of CH_4, it mainly comes from the alloying, metal redispersion, and oxide/metal interface formation. A metallic active species is beneficial for CH_4 production. Moreover, chemical phase transformation in some cases facilitates the improvement of C_{2+} product (especially light olefins) selectivity, which results from more active structures with C−C coupling ability, such as $ZnFeO_4$ spinel, Co_2C, and Fe_5C_2.

Stability is another important indicator for evaluating the catalytic performance. Structural evolution during the reaction process is often accompanied by changes in the catalyst stability. Two possible processes affect the stability. On the one hand, the catalyst causes a transient or metastable reconstruction. These short-lived, nonequilibrium structures may be crucial for activity but are prone to further evolution over longer time scales (e.g., specific surface adsorbate layers or subsurface oxygen species that may lead to slow restructuring or deactivation). In this case, it is highly expected that the active metastable structure can be stabilized using catalyst design through the interface confinement effect. On the other hand, the catalyst goes through an adaptive or self-stabilizing evolution. Transformations that drive the system toward a thermodynamically stable or kinetically trapped active state under steady-state reaction conditions due to the intrinsic interface confinement effect and environment atmosphere confinement (e.g., formation of a stable metal carbide phase or an equilibrated metal−support interface). In this case, *operando* or *in situ* characterizations combined with *ex situ* results on time scales must be critically assessed against catalyst lifetime to differentiate between these categories. Furthermore, the reversibility affects the stability of dynamically formed structures, which mainly depends on the reaction microenvironment, especially gas compositions. The kinetic trapping of structural evolution through *operando* or *in situ* characterizations and further stabilization for the active structure will help the dynamic behavior of catalysts go from phenomenon description to the mechanism and control level. Overall, by utilizing the interface confinement effect and the ambient atmosphere to stabilize the active structures during the reaction, it can achieve a controllable tuning of catalytic performance.

4. SUMMARY AND OUTLOOK

In summary, the dynamic evolution of catalyst structures under reaction conditions involves surface/interface reconstruction and chemical phase transformations. The chemical potential of the gas phase dictates the thermodynamic direction (oxidation, reduction, and others). Surface atoms of the catalyst go through oxidation by molecules like CO_2 and H_2O, reduction by molecules like CO and H_2, carburization by $HCOO^-$ and CO, or the formation of a complex with reaction molecules (such as M-OH, M-CO, M-CO_2 or M-CHO_x) through the effects of the reaction microenvironment. Such reactions drive atomic diffusion, migration, and reconstruction on the catalyst, removal from the catalyst, or addition or exchange from reaction atmospheres to the catalyst. A more stable structure is prone to form during the reaction via a self-optimization strategy. Multiple reaction processes determine the final active structure. For example, the formation of carbide relies on the oxidation/reduction and subsequent carburization process.

Importantly, the dynamic evolutions bring about more active structures for CO_2 conversion, such as oxide/metal and oxide/oxide interfaces, coordinatively unsaturated sites or vacancies, solid solutions or spinels, and carbide. The new structures show changes in several aspects to enhance catalytic performance (increased CO_2 conversion, altered product selectivity, and promoted catalyst stability) in CO_2 hydrogenation, including promoted adsorption and dissociation ability of CO_2 or H_2, altered adsorption strength of the reaction intermediate, optimized electronic structures for efficient charge transfer, and the opening of alternative reaction pathways with lower

https://doi.org/10.1021/jacsau.5c01671
JACS Au XXXX, XXX, XXX−XXX

activation energy barriers, thereby simultaneously boosting catalytic activity and product selectivity.

Two interaction modes, SMSI and SOSI, are the keys to forming oxide/metal and oxide/oxide interface structures, significantly optimizing the catalyst structure and promoting activity. Due to the high activity of oxide/metal interface structures, constructing oxide/metal reverse catalysts to obtain more interface active sites needs to receive increasing attention. The reconstruction of alloying or dealloying for bimetallic catalysts and the formation of solid solutions or spinels for oxide complexes that form more active catalytic sites are also highly anticipated to be developed. Additionally, the positive feedback mechanism where carburization by reaction products enhances catalytic activity in CO_2 hydrogenation is another phenomenon worthy of focus, particularly for transition metals like Fe, Co, Ni, and Mo, which show outstanding catalytic activity and altered product selectivity after carburization.

Despite numerous advances in dynamic structural evolution, most of which are beneficial for CO_2 conversion, there are some cases where this is not the case. For example, over-encapsulation due to SMSI may lead to loss of accessible active sites, decreasing catalytic activity. The formation of the oxide/metal or oxide/oxide interface may also bring about mass-transport limitations. The catalyst may undergo long-term degradation due to cyclic processes (redox reactions, oxidation/carburization), leading to fatigue, crack formation, and phase separation. Therefore, a critical balance between strength and limitations is crucial to avoid unfavorable structural evolution for CO_2 conversion.

For future research on the dynamic evolution of catalyst structures under CO_2 hydrogenation conditions, several aspects deserve attention:

(1) **Deepening the understanding of surface reconstruction mechanisms.** By utilizing rapidly developing *in situ* characterization techniques such as *in situ* environmental transmission electron microscopy and X-ray absorption spectroscopy, the mechanisms of surface atom migration and reconstruction need to be further investigated under realistic reaction conditions. Identifying the key factors governing structural evolution will help reveal real-time dynamic processes and enable precise control over surface restructuring.

(2) **Developing multitechnology correlation methods.** While *operando* and *in situ* characterization have transformed our understanding of catalyst kinetics, their inherent limitations must be recognized to guide future methodological developments. Key challenges include (i) probe-induced effects, such as localized structural and compositional changes induced by electron beams or intense X-rays; (ii) the pressure and environmental gaps between ideal measurement conditions and actual reactor environments; and (iii) the ongoing trade-offs between temporal, spatial, and spectral resolutions. Therefore, multitechnology correlation methods remain crucial. Crucially, detailed *ex situ* analysis of spent catalysts can provide supplementary information on their final structural state. By correlating insights from *in situ* experiments with high-resolution postreaction characterization results, we can validate kinetic models and bridge gaps in our understanding of mechanisms. Future progress hinges on two aspects: first, advancing *in situ* methods to conditions closer to reality, and second, intelligently integrating all available observation windows into a coherent picture of the catalyst lifecycle.

(3) **Designing efficient and stable reverse catalysts.** It is promising to design and optimize oxide/metal reverse catalysts with more oxide/metal interface active sites, explore a broader range of oxide and metal combinations based on the selectivity of different metals or oxides toward specific products, and tune the interface structures and properties with improved CO_2 hydrogenation activity and stability, as well as the yield of high-value-added products.

(4) **Developing*in situ*redispersion catalysts.** Oxide catalysts usually show relatively weak activity in CO_2 hydrogenation. The construction of highly active interfaces with more coordinatively unsaturated sites is crucial via the dispersion and migration of oxides during the reaction. The combination of redispersed oxide and metal is also of considerable interest to enhance CO_2 hydrogenation activity.

(5) **Exploring reaction-induced chemical phase transformation phenomena.** It is important to investigate the factors affecting catalyst phase transitions, especially the dynamics and equilibrium of chemical phase transformation under different reaction conditions, achieve controllable regulation of catalyst phase transformation, and develop catalysts with adaptive and highly stable properties. Additionally, it is significant to couple the properties of both oxides and carbides in CO_2 hydrogenation by adjusting the carburization degree of oxide, which enables sequential reactions from CO_2 to intermediates (e.g., CO) and then to other high-value-added products (e.g., higher alcohols, olefins, etc.).

(6) **Multiscale simulation and theoretical calculations.** Multiscale simulations and theoretical calculations can be used to gain deep insights into the appropriate structural evolution and dynamic mechanisms of catalysts during reactions. Doing so would provide theoretical guidance for the design and optimization of highly efficient and stable catalysts, further improving the performance of catalysts in CO_2 hydrogenation.

AUTHOR INFORMATION

Corresponding Author

Qiang Fu − *State Key Laboratory of Catalysis, Dalian Institute of Chemical Physics, Chinese Academy of Sciences, Dalian 116023, China;* orcid.org/0000-0001-5316-6758; Email: qfu@dicp.ac.cn

Authors

Xiangze Du − *State Key Laboratory of Catalysis, Dalian Institute of Chemical Physics, Chinese Academy of Sciences, Dalian 116023, China; Max Planck-Cardiff Centre on the Fundamentals of Heterogeneous Catalysis FUNCAT, Translational Research Hub, Cardiff University, Cardiff CF24 4HQ, U.K.*

Yamei Fan − *State Key Laboratory of Catalysis, Dalian Institute of Chemical Physics, Chinese Academy of Sciences, Dalian 116023, China; Max Planck-Cardiff Centre on the Fundamentals of Heterogeneous Catalysis FUNCAT, Translational Research Hub, Cardiff University, Cardiff CF24 4HQ, U.K.*

https://doi.org/10.1021/jacsau.5c01671
JACS Au XXXX, XXX, XXX−XXX

Jun Fan − *State Key Laboratory of Catalysis, Dalian Institute of Chemical Physics, Chinese Academy of Sciences, Dalian 116023, China*
Xiaoyue Wang − *State Key Laboratory of Catalysis, Dalian Institute of Chemical Physics, Chinese Academy of Sciences, Dalian 116023, China*
Rongtan Li − *State Key Laboratory of Catalysis, Dalian Institute of Chemical Physics, Chinese Academy of Sciences, Dalian 116023, China;* orcid.org/0000-0003-2061-3368
Wenjing Bao − *State Key Laboratory of Catalysis, Dalian Institute of Chemical Physics, Chinese Academy of Sciences, Dalian 116023, China*

Complete contact information is available at: https://pubs.acs.org/10.1021/jacsau.5c01671

Notes

The authors declare no competing financial interest.

■ ACKNOWLEDGMENTS

This work is supported by the National Key R&D Program of China (2023YFA1506600), the National Natural Science Foundation of China (22402195, 22332006, 22288201, and 22321002), the Photon Science Center for Carbon Neutrality, and the Fundamental Research Funds for the Central Universities (207202550005).

■ REFERENCES

(1) Liu, L.; Corma, A. Evolution of Isolated Atoms and Clusters in Catalysis. *Trends Chem.* **2020**, *2* (4), 383−400.
(2) Liu, L.; Corma, A. Structural transformations of solid electrocatalysts and photocatalysts. *Nat. Rev. Chem.* **2021**, *5* (4), 256−276.
(3) Newton, M. A. Dynamic adsorbate reaction induced structural change of supported metal nanoparticles heterogeneous catalysis and beyond. *Chem. Soc. Rev.* **2008**, *37*, 2644−2657.
(4) Tang, M.; Yuan, W.; Ou, Y.; Li, G.; You, R.; Li, S.; Yang, H.; Zhang, Z.; Wang, Y. Recent Progresses on Structural Reconstruction of Nanosized Metal Catalysts via Controlled-Atmosphere Transmission Electron Microscopy: A Review. *ACS Catal.* **2020**, *10* (24), 14419−14450.
(5) Lv, H.; Guo, W.; Chen, M.; Zhou, H.; Wu, Y. Rational construction of thermally stable single atom catalysts: From atomic structure to practical applications. *Chin. J. Catal.* **2022**, *43* (1), 71−91.
(6) Ye, R.; Ding, J.; Reina, T. R.; Duyar, M. S.; Li, H.; Luo, W.; Zhang, R.; Fan, M.; Feng, G.; Sun, J.; Liu, J. Design of catalysts for selective CO_2 hydrogenation. *Nat. Synth.* **2025**, *4* (3), 288−302.
(7) Zhou, H.; Chen, Z.; Kountoupi, E.; Tsoukalou, A.; Abdala, P. M.; Florian, P.; Fedorov, A.; Müller, C. R. Two-dimensional molybdenum carbide 2D-Mo_2C as a superior catalyst for CO_2 hydrogenation. *Nat. Commun.* **2021**, *12* (1), 5510.
(8) Rezvani, A.; Abdel-Mageed, A. M.; Ishida, T.; Murayama, T.; Parlinska-Wojtan, M.; Behm, R. J. CO_2 Reduction to Methanol on Au/CeO_2 Catalysts: Mechanistic Insights from Activation/Deactivation and SSITKA Measurements. *ACS Catal.* **2020**, *10* (6), 3580−3594.
(9) Fan, Y.; Wang, F.; Li, R.; Liu, C.; Fu, Q. Surface Hydroxyl-Determined Migration and Anchoring of Silver on Alumina in Oxidative Redispersion. *ACS Catal.* **2023**, *13* (4), 2277−2285.
(10) Lu, S.; Yang, H.; Zhou, Z.; Zhong, L.; Li, S.; Gao, P.; Sun, Y. Effect of In_2O_3 particle size on CO_2 hydrogenation to lower olefins over bifunctional catalysts. *Chin. J. Catal.* **2021**, *42* (11), 2038−2048.
(11) Han, B.; Li, Q.; Jiang, X.; Guo, Y.; Jiang, Q.; Su, Y.; Li, L.; Qiao, B. Switchable Tuning CO_2 Hydrogenation Selectivity by Encapsulation of the Rh Nanoparticles While Exposing Single Atoms. *Small* **2022**, *18* (45), No. e2204490.
(12) Xia, G.-J.; Lee, M.-S.; Glezakou, V.-A.; Rousseau, R.; Wang, Y.-G. Diffusion and Surface Segregation of Interstitial Ti Defects Induced by Electronic Metal-Support Interactions on a Au/TiO_2 Nanocatalyst. *ACS Catal.* **2022**, *12* (8), 4455−4464.
(13) Zhang, Y.; Hu, A.; Xia, D.; Hwang, S.; Sainio, S.; Nordlund, D.; Michel, F. M.; Moore, R. B.; Li, L.; Lin, F. Operando characterization and regulation of metal dissolution and redeposition dynamics near battery electrode surface. *Nat. Nanotechnol.* **2023**, *18* (7), 790−797.
(14) Mohammadi Aframehr, W.; Pfromm, P. H. Activating dinitrogen for chemical looping ammonia synthesis: nitridation of manganese. *J. Mater. Sci.* **2021**, *56* (22), 12584−12595.
(15) Xin, H.; Li, R.; Lin, L.; Mu, R.; Li, M.; Li, D.; Fu, Q.; Bao, X. Reverse water gas-shift reaction product driven dynamic activation of molybdenum nitride catalyst surface. *Nat. Commun.* **2024**, *15* (1), 3100.
(16) Bao, X. The 'energy revolution'calls for technological innovation. *Nat. Sci. Rev.* **2022**, *9*, nwac117.
(17) Zhang, X.; Han, S.; Zhu, B.; Zhang, G.; Li, X.; Gao, Y.; Wu, Z.; Yang, B.; Liu, Y.; Baaziz, W.; Ersen, O.; Gu, M.; Miller, J. T.; Liu, W. Reversible loss of core-shell structure for Ni-Au bimetallic nanoparticles during CO_2 hydrogenation. *Nat. Catal.* **2020**, *3* (4), 411−417.
(18) Sun, Q.; Liu, X.; Gu, Q.; Sun, Z.; Wang, H.; Cao, L.; Xu, Y.; Li, S.; Yang, B.; Wei, S.; Lu, J. Breaking the Conversion-Selectivity Trade-Off in Methanol Synthesis from CO_2 Using Dual Intimate Oxide/Metal Interfaces. *J. Am. Chem. Soc.* **2024**, *146* (42), 28885−28894.
(19) Araujo, T. P.; Morales-Vidal, J.; Giannakakis, G.; Mondelli, C.; Eliasson, H.; Erni, R.; Stewart, J. A.; Mitchell, S.; Lopez, N.; Perez-Ramirez, J. Reaction-Induced Metal-Metal Oxide Interactions in Pd-In_2O_3/ZrO_2 Catalysts Drive Selective and Stable CO_2 Hydrogenation to Methanol. *Angew. Chem., Int. Ed.* **2023**, *62* (42), No. e202306563.
(20) Lee, S. W.; Luna, M. L.; Berdunov, N.; Wan, W.; Kunze, S.; Shaikhutdinov, S.; Cuenya, B. R. Unraveling surface structures of gallium promoted transition metal catalysts in CO_2 hydrogenation. *Nat. Commun.* **2023**, *14* (1), 4649.
(21) Liu, Y.; Zhang, G.; Liu, S.; Zhu, J.; Liu, J.; Wang, J.; Li, R.; Wang, M.; Fu, Q.; Hou, S.; Song, C.; Guo, X. Promoting *n*-Butane Dehydrogenation over PtMn/SiO_2 through Structural Evolution Induced by a Reverse Water-Gas Shift Reaction. *ACS Catal.* **2022**, *12* (21), 13506−13512.
(22) Alayoglu, S.; Beaumont, S. K.; Zheng, F.; Pushkarev, V. V.; Zheng, H.; Iablokov, V.; Liu, Z.; Guo, J.; Kruse, N.; Somorjai, G. A. CO_2 Hydrogenation Studies on Co and CoPt Bimetallic Nanoparticles Under Reaction Conditions Using TEM, XPS and NEXAFS. *Top. Catal.* **2011**, *54* (13−15), 778−785.
(23) Muller, A.; Comas-Vives, A.; Coperet, C. Ga and Zn increase the oxygen affinity of Cu-based catalysts for the CO_x hydrogenation according to ab initio atomistic thermodynamics. *Chem. Sci.* **2022**, *13* (45), 13442−13458.
(24) Wu, G.; Liu, Y.; Wang, J. Oxidative-Atmosphere-Induced Strong Metal-Support Interaction and Its Catalytic Application. *Acc. Chem. Res.* **2023**, *56* (8), 911−923.
(25) Luo, Z.; Zhao, G.; Pan, H.; Sun, W. Strong Metal-Support Interaction in Heterogeneous Catalysts. *Adv. Energy Mater.* **2022**, *12* (37), 2201395.
(26) Wang, H.; Wang, L.; Xiao, F.-S. New routes for the construction of strong metal-support interactions. *Sci. China Chem.* **2022**, *65* (11), 2051−2057.
(27) Pu, T.; Zhang, W.; Zhu, M. Engineering Heterogeneous Catalysis with Strong Metal-Support Interactions: Characterization, Theory and Manipulation. *Angew. Chem., Int. Ed.* **2023**, *62* (4), No. e202212278.
(28) Monai, M.; Jenkinson, K.; Melcherts, A. E.; Louwen, J. N.; Irmak, E. A.; Van Aert, S.; Altantzis, T.; Vogt, C.; van der Stam, W.; Duchoň, T.; Šmíd, B.; Groeneveld, E.; Berben, P.; Bals, S.; Weckhuysen, B. M. Restructuring of titanium oxide overlayers over nickel nanoparticles during catalysis. *Science* **2023**, *380* (6645), 644−651.
(29) Xin, H.; Lin, L.; Li, R.; Li, D.; Song, T.; Mu, R.; Fu, Q.; Bao, X. Overturning CO_2 Hydrogenation Selectivity with High Activity via Reaction-Induced Strong Metal-Support Interactions. *J. Am. Chem. Soc.* **2022**, *144* (11), 4874−4882.
(30) Zhang, W.; Lin, H.; Wei, Y.; Zhou, X.; An, Y.; Dai, Y.; Niu, Q.; Lin, T.; Zhong, L. Overturning CO_2 Hydrogenation Selectivity via

Strong Metal-Support Interaction. *ACS Catal.* **2024**, *14* (4), 2409−2417.
(31) Song, T.; Li, R.; Wang, J.; Dong, C.; Feng, X.; Ning, Y.; Mu, R.; Fu, Q. Enhanced Methanol Synthesis over Self-Limited ZnO_x Overlayers on Cu Nanoparticles Formed via Gas-Phase Migration Route. *Angew. Chem., Int. Ed.* **2024**, *63* (5), No. e202316888.
(32) Wang, H.; Wang, L.; Lin, D.; Feng, X.; Niu, Y.; Zhang, B.; Xiao, F.-S. Strong metal-support interactions on gold nanoparticle catalysts achieved through Le Chatelier's principle. *Nat. Catal.* **2021**, *4* (5), 418−424.
(33) Wu, C.; Lin, L.; Liu, J.; Zhang, J.; Zhang, F.; Zhou, T.; Rui, N.; Yao, S.; Deng, Y.; Yang, F.; Xu, W.; Luo, J.; Zhao, Y.; Yan, B.; Wen, X.-D.; Rodriguez, J. A.; Ma, D. Inverse ZrO_2/Cu as a highly efficient methanol synthesis catalyst from CO_2 hydrogenation. *Nat. Commun.* **2020**, *11* (1), 5767.
(34) Matsubu, J. C.; Zhang, S.; DeRita, L.; Marinkovic, N. S.; Chen, J. G.; Graham, G. W.; Pan, X.; Christopher, P. Adsorbate-mediated strong metal-support interactions in oxide-supported Rh catalysts. *Nat. Chem.* **2017**, *9* (2), 120−127.
(35) Li, J.; Zhang, L.; An, X.; Feng, K.; Wang, X.; He, J.; Huang, Y.; Liu, J.; Zhang, L.; Yan, B.; Li, C.; He, L. Tuning Adsorbate-Mediated Strong Metal-Support Interaction by Oxygen Vacancy: A Case Study in Ru/TiO_2. *Angew. Chem., Int. Ed.* **2024**, *63* (31), No. e202407025.
(36) Zhang, W.; Li, D.; Liu, C.; Jiang, Z.; Gao, C.; Shen, L.; Liu, Q.; Qiu, R.; Gu, H.; Lian, C.; Xu, J.; Zhu, M. Facilitated CO_2 hydrogenation by strong metal-support interaction between Ni and $BaCO_3$. *Chem. Catal.* **2024**, *4* (10), 101113.
(37) Liu, X.; Luo, J.; Wang, H.; Huang, L.; Wang, S.; Li, S.; Sun, Z.; Sun, F.; Jiang, Z.; Wei, S.; Li, W. X.; Lu, J. In Situ Spectroscopic Characterization and Theoretical Calculations Identify Partially Reduced ZnO_{1-x}/Cu Interfaces for Methanol Synthesis from CO_2. *Angew. Chem., Int. Ed.* **2022**, *61* (23), No. e202202330.
(38) Reichenbach, T.; Mondal, K.; Jäger, M.; Vent-Schmidt, T.; Himmel, D.; Dybbert, V.; Bruix, A.; Krossing, I.; Walter, M.; Moseler, M. Ab initio study of CO_2 hydrogenation mechanisms on inverse ZnO/Cu catalysts. *J. Catal.* **2018**, *360*, 168−174.
(39) Xiong, W.; Wu, Z.; Chen, X.; Ding, J.; Ye, A.; Zhang, W.; Huang, W. Active copper structures in ZnO-Cu interfacial catalysis: CO_2 hydrogenation to methanol and reverse water-gas shift reactions. *Sci. China Chem.* **2024**, *67* (2), 715−723.
(40) Xu, Y.; Wang, M.; Xie, Z.; Tian, D.; Sheng, G.; Tang, X.; Li, H.; Wu, Y.; Song, C.; Gao, X.; Yao, S.; Ma, D.; Lin, L. Insights into the interfacial structure of Cu/ZrO_2 catalysts for methanol synthesis from CO_2 hydrogenation: Effects of Cu-supported nano-ZrO_2 inverse interface. *Chem. Eng. J.* **2023**, *470*, 144006.
(41) Wang, M.; Xu, Y.; Tang, H.; Tian, S.; Zeng, L.; Li, H.; Wu, C.; Hu, Z.; Su, M.; Zheng, H.; Wang, M.; Ma, D. Optimizing methanol synthesis from CO_2 hydrogenation over inverse Zr-Cu catalyst. *Chem. Catal.* **2024**, *4* (5), 100985.
(42) Kumari, S.; Alexandrova, A. N.; Sautet, P. Nature of Zirconia on a Copper Inverse Catalyst Under CO_2 Hydrogenation Conditions. *J. Am. Chem. Soc.* **2023**, *145* (48), 26350−26362.
(43) Xu, Y.; Gao, Z.; Xu, Y.; Qin, X.; Tang, X.; Xie, Z.; Zhang, J.; Song, C.; Yao, S.; Zhou, W.; Ma, D.; Lin, L. Cu-supported nano-$ZrZnO_x$ as a highly active inverse catalyst for low temperature methanol synthesis from CO_2 hydrogenation. *Appl. Catal., B* **2024**, *344*, 123656.
(44) Zou, T.; Araújo, T. P.; Krumeich, F.; Mondelli, C.; Pérez-Ramírez, J. ZnO-Promoted Inverse ZrO_2-Cu Catalysts for CO_2-Based Methanol Synthesis under Mild Conditions. *ACS Sustainable Chem. Eng.* **2022**, *10* (1), 81−90.
(45) Moncada, J.; Chen, X.; Deng, K.; Wang, Y.; Xu, W.; Marinkovic, N.; Zhou, G.; Martínez-Arias, A.; Rodriguez, J. A. Structural and Chemical Evolution of an Inverse CeO_x/Cu Catalyst under CO_2 Hydrogenation: Tuning Oxide Morphology to Improve Activity and Selectivity. *ACS Catal.* **2023**, *13* (23), 15248−15258.
(46) Yang, H.; Geng, X.; Yang, Y.; Li, Y.-W.; Wen, X.-D.; Jiao, H. Interface mediated CO_2 hydrogenation on inverse supported ZrO_2/Ni(111) nanocluster catalyst. *Appl. Surf. Sci.* **2024**, *642*, 158562.
(47) Zhu, Y.; Luo, R.; Shi, H.; Koh, K.; Kovarik, L.; Fulton, J. L.; Lercher, J. A.; Zhao, Z.-J.; Gong, J.; Gutiérrez, O. Y. Formation of (Rh-Fe)-FeO_x Complex Sites Enables Methanol Synthesis from CO_2. *ACS Catal.* **2024**, *14* (13), 10031−10039.
(48) Tang, X.; Song, C.; Li, H.; Liu, W.; Hu, X.; Chen, Q.; Lu, H.; Yao, S.; Li, X.-n.; Lin, L. Thermally stable Ni foam-supported inverse $CeAlO_x$/Ni ensemble as an active structured catalyst for CO_2 hydrogenation to methane. *Nat. Commun.* **2024**, *15* (1), 3115.
(49) Salvatore, K. L.; Deng, K.; Yue, S.; McGuire, S. C.; Rodriguez, J. A.; Wong, S. S. Optimized Microwave-Based Synthesis of Thermally Stable Inverse Catalytic Core-shell Motifs for CO_2 Hydrogenation. *ACS Appl. Mater. Interfaces* **2020**, *12* (29), 32591−32603.
(50) Wang, H.; Zhou, H.; Li, S.; Ge, X.; Wang, L.; Jin, Z.; Wang, C.; Ma, J.; Chu, X.; Meng, X.; Zhang, W.; Xiao, F.-S. Strong Oxide-Support Interactions Accelerate Selective Dehydrogenation of Propane by Modulating the Surface Oxygen. *ACS Catal.* **2020**, *10* (18), 10559−10569.
(51) Jaegers, N. R.; Danghyan, V.; Shangguan, J.; Lizandara-Pueyo, C.; Deshlahra, P.; Iglesia, E. Heterolytic C-H Activation Routes in Catalytic Dehydrogenation of Light Alkanes on Lewis Acid-Base Pairs at ZrO_2 Surfaces. *J. Am. Chem. Soc.* **2024**, *146* (37), 25710−25726.
(52) Jiao, F.; Bai, B.; Li, G.; Pan, X.; Ye, Y.; Qu, S.; Xu, C.; Xiao, J.; Jia, Z.; Liu, W.; et al. Disentangling the activity-selectivity trade-off in catalytic conversion of syngas to light olefins. *Science* **2023**, *380* (6646), 727−730.
(53) Wang, M.; Zheng, L.; Wang, G.; Cui, J.; Guan, G.-L.; Miao, Y.-T.; Wu, J.-F.; Gao, P.; Yang, F.; Ling, Y.; Luo, X.; Zhang, Q.; Fu, G.; Cheng, K.; Wang, Y. Spinel Nanostructures for the Hydrogenation of CO_2 to Methanol and Hydrocarbon Chemicals. *J. Am. Chem. Soc.* **2024**, *146* (21), 14528−14538.
(54) Li, Y.; Zhao, Z.; Zhao, M.; Zhu, H.; Ma, X.; Li, Z.; Lu, W.; Chen, X.; Ying, L.; Lin, R.; Meng, Y.; Lyu, Y.; Yan, L.; Ding, Y. Oxygen-vacancy induced structural changes of Co species in $CoAl_2O_4$ spinels for CO_2 hydrogenation. *Appl. Catal., B* **2024**, *347*, 123824.
(55) Dang, S.; Qin, B.; Yang, Y.; Wang, H.; Cai, J.; Han, Y.; Li, S.; Gao, P.; Sun, Y. Rationally designed indium oxide catalysts for CO_2 hydrogenation to methanol with high activity and selectivity. *Sci. Adv.* **2020**, *6* (25), No. eaaz2060.
(56) Nguyen, T. X.; Liao, Y. C.; Lin, C. C.; Su, Y. H.; Ting, J. M. Advanced High Entropy Perovskite Oxide Electrocatalyst for Oxygen Evolution Reaction. *Adv. Funct. Mater.* **2021**, *31* (27), 2101632.
(57) Zheng, X.; Qin, M.; Ma, S.; Chen, Y.; Ning, H.; Yang, R.; Mao, S.; Wang, Y. Strong Oxide-Support Interaction over IrO_2/V_2O_5 for Efficient pH-Universal Water Splitting. *Adv. Sci.* **2022**, *9* (11), 2104636.
(58) Dai, J.; Zhu, Y.; Chen, Y.; Wen, X.; Long, M.; Wu, X.; Hu, Z.; Guan, D.; Wang, X.; Zhou, C.; Lin, Q.; Sun, Y.; Weng, S.-C.; Wang, H.; Zhou, W.; Shao, Z. Hydrogen spillover in complex oxide multifunctional sites improves acidic hydrogen evolution electrocatalysis. *Nat. Commun.* **2022**, *13* (1), 1189.
(59) Li, C.; Jang, H.; Kim, M. G.; Hou, L.; Liu, X.; Cho, J. Ru-incorporated oxygen-vacancy-enriched MoO_2 electrocatalysts for hydrogen evolution reaction. *Appl. Catal., B* **2022**, *307*, 121204.
(60) Wachs, I. E.; Saleh, R. Y.; Chan, S. S.; Chersich, C. C. The interaction of vanadium pentoxide with titania (anatase): Part I. Effect on o-xylene oxidation to phthalic anhydride. *Appl. Catal.* **1985**, *15* (2), 339−352.
(61) Bond, G. C.; Tahir, S. F. Vanadium oxide monolayer catalysts: Preparation, characterization and catalytic activity. *Appl. Catal.* **1991**, *71* (1), 1−31.
(62) Dong, C.; Mu, R.; Li, R.; Wang, J.; Song, T.; Qu, Z.; Fu, Q.; Bao, X. Disentangling Local Interfacial Confinement and Remote Spillover Effects in Oxide-Oxide Interactions. *J. Am. Chem. Soc.* **2023**, *145* (31), 17056−17065.
(63) Ahmadi Khoshooei, M.; Wang, X.; Vitale, G.; Formalik, F.; Kirlikovali, K. O.; Snurr, R. Q.; Pereira-Almao, P.; Farha, O. K. An active, stable cubic molybdenum carbide catalyst for the high-temperature reverse water-gas shift reaction. *Science* **2024**, *384* (6695), 540−546.

https://doi.org/10.1021/jacsau.5c01671
JACS Au XXXX, XXX, XXX−XXX

(64) Zhang, M.; Chen, H.; Cheng, K.; Zhao, L.; Huang, H.; Kang, J.; Zhang, Q.; Wang, Y. Reaction-Induced Formation of CoO_x-InO_x Interfaces for the Hydrogenation of CO_2 to Methanol. *J. Phys. Chem. C* **2025**, *129* (5), 2535−2545.
(65) Meng, S.; Wu, L.; Liu, M.; Cui, Z.; Chen, Q.; Li, S.; Yan, J.; Wang, L.; Wang, X.; Qian, J.; Guo, H.; Niu, J.; Bogaerts, A.; Yi, Y. Plasma-driven CO_2 hydrogenation to CH_3OH over Fe_2O_3/γ-Al_2O_3 catalyst. *AIChE J.* **2023**, *69* (10), No. e18154.
(66) Zhang, X.; Zhang, G.; Liu, W.; Yuan, F.; Wang, J.; Zhu, J.; Jiang, X.; Zhang, A.; Ding, F.; Song, C.; Guo, X. Reaction-driven surface reconstruction of $ZnAl_2O_4$ boosts the methanol selectivity in CO_2 catalytic hydrogenation. *Appl. Catal., B* **2021**, *284*, 119700.
(67) Zhang, X.; Zhang, G.; Zhou, X.; Wang, Z.; Liu, Y.; Zhu, J.; Song, C.; Guo, X. Identification of the Active Sites on ZnO/ZrO_2 for CO_2 Hydrogenation to CO and Methanol. *Ind. Eng. Chem. Res.* **2023**, *62* (49), 21173−21181.
(68) Zhang, X.; Kirilin, A. V.; Rozeveld, S.; Kang, J. H.; Pollefeyt, G.; Yancey, D. F.; Chojecki, A.; Vanchura, B.; Blum, M. Support Effect and Surface Reconstruction in In_2O_3/m-ZrO_2 Catalyzed CO_2 Hydrogenation. *ACS Catal.* **2022**, *12* (7), 3868−3880.
(69) Ouyang, T.; Jin, B.; Mao, Y.; Wei, D.; Liang, Z. Control of strong electronic oxide-support interaction in iron-based redox catalysts for highly efficient chemical looping CO_2 conversion. *Appl. Catal., B* **2024**, *343*, 123531.
(70) Rui, N.; Wang, X.; Deng, K.; Moncada, J.; Rosales, R.; Zhang, F.; Xu, W.; Waluyo, I.; Hunt, A.; Stavitski, E.; Senanayake, S. D.; Liu, P.; Rodriguez, J. A. Atomic Structural Origin of the High Methanol Selectivity over In_2O_3-Metal Interfaces: Metal-Support Interactions and the Formation of a InO_x Overlayer in Ru/In_2O_3 Catalysts during CO_2 Hydrogenation. *ACS Catal.* **2023**, *13* (5), 3187−3200.
(71) Kelemen, S. R.; Freund, H. XPS characterization of glassy-carbon surfaces oxidized by O_2, CO_2, and HNO_3. *Energy Fuels* **1988**, *2* (2), 111−118.
(72) Bowden, B.; Davies, M.; Davies, P. R.; Guan, S.; Morgan, D. J.; Roberts, V.; Wotton, D. The deposition of metal nanoparticles on carbon surfaces: the role of specific functional groups. *Faraday Discuss.* **2018**, *208*, 455−470.
(73) Li, M.; Borsay, A.; Dakhchoune, M.; Zhao, K.; Luo, W.; Züttel, A. Thermal stability of size-selected copper nanoparticles: Effect of size, support and CO_2 hydrogenation atmosphere. *Appl. Surf. Sci.* **2020**, *510*, 145439.
(74) Ma, J.; Xu, B.; Cao, S.; Li, S.; Chu, W.; Perathoner, S.; Centi, G.; Liu, Y. Structural dynamics of Ni/Mo_2CT MXene catalysts under reaction modulate CO_2 reduction performance. *Chin. J. Catal.* **2025**, *72*, 243−253.
(75) Phongprueksathat, N.; Ting, K. W.; Mine, S.; Jing, Y.; Toyoshima, R.; Kondoh, H.; Shimizu, K.-i.; Toyao, T.; Urakawa, A. Bifunctionality of Re Supported on TiO_2 in Driving Methanol Formation in Low-Temperature CO_2 Hydrogenation. *ACS Catal.* **2023**, *13* (16), 10734−10750.
(76) Bando, K. K.; Ichikuni, N.; Soga, K.; Kunimori, K.; Arakawa, H.; Asakura, K. Characterization of Rh Particles and Li-Promoted Rh Particles in Y Zeolite during CO_2 Hydrogenation—A New Mechanism for Catalysis Controlled by the Dynamic Structure of Rh Particles and the Li Additive Effect. *J. Catal.* **2000**, *194* (1), 91−104.
(77) Fan, Y.; Li, R.; Wang, B.; Feng, X.; Du, X.; Liu, C.; Wang, F.; Liu, C.; Dong, C.; Ning, Y.; Mu, R.; Fu, Q. Water-assisted oxidative redispersion of Cu particles through formation of Cu hydroxide at room temperature. *Nat. Commun.* **2024**, *15* (1), 3046.
(78) Liu, L.; Lu, J.; Yang, Y.; Ruettinger, W.; Gao, X.; Wang, M.; Lou, H.; Wang, Z.; Liu, Y.; Tao, X.; et al. Dealuminated Beta zeolite reverses Ostwald ripening for durable copper nanoparticle catalysts. *Science* **2024**, *383* (6678), 94−101.
(79) Yang, C.; Pei, C.; Luo, R.; Liu, S.; Wang, Y.; Wang, Z.; Zhao, Z.-J.; Gong, J. Strong Electronic Oxide-Support Interaction over In_2O_3/ZrO_2 for Highly Selective CO_2 Hydrogenation to Methanol. *J. Am. Chem. Soc.* **2020**, *142* (46), 19523−19531.
(80) Wang, J.; Li, R.; Zhang, G.; Dong, C.; Fan, Y.; Yang, S.; Chen, M.; Guo, X.; Mu, R.; Ning, Y.; Li, M.; Fu, Q.; Bao, X. Confinement-Induced Indium Oxide Nanolayers Formed on Oxide Support for Enhanced CO_2 Hydrogenation Reaction. *J. Am. Chem. Soc.* **2024**, *146* (8), 5523−5531.
(81) Eliasson, H.; Chiang, Y. T.; Araujo, T. P.; Li, X.; Erni, R.; Mitchell, S.; Perez-Ramirez, J. Tracking Dynamics of Supported Indium Oxide Catalysts in CO_2 Hydrogenation to Methanol by In Situ TEM. *Adv. Mater.* **2025**, *37* (20), No. e2419859.
(82) Kang, H.; Zhu, L.; Li, S.; Yu, S.; Niu, Y.; Zhang, B.; Chu, W.; Liu, X.; Perathoner, S.; Centi, G.; Liu, Y. Generation of oxide surface patches promoting H-spillover in Ru/(TiO_x)MnO catalysts enables CO_2 reduction to CO. *Nat. Catal.* **2023**, *6* (11), 1062−1072.
(83) Deng, K.; Wang, Y.; Perez-Bailac, P.; Xu, W.; Llorca, J.; Martinez-Arias, A.; Zakharov, D. N.; Rodriguez, J. A. Visualizing Size-Dependent Dynamics of $CeO_{2-\delta}${100}-Supported CoO_x Nanoparticles Under CO_2 Hydrogenation Conditions. *J. Am. Chem. Soc.* **2025**, *147* (22), 19239−19252.
(84) Yang, M.; Yu, J.; Zimina, A.; Sarma, B. B.; Pandit, L.; Grunwaldt, J. D.; Zhang, L.; Xu, H.; Sun, J. Probing the Nature of Zinc in Copper-Zinc-Zirconium Catalysts by Operando Spectroscopies for CO_2 Hydrogenation to Methanol. *Angew. Chem., Int. Ed.* **2023**, *62* (7), No. e202216803.
(85) Zhang, X.; Yu, X.; Mendes, R. G.; Matvija, P.; Melcherts, A. E. M.; Sun, C.; Ye, X.; Weckhuysen, B. M.; Monai, M. Highly Dispersed ZnO Sites in a ZnO/ZrO_2 Catalyst Promote Carbon Dioxide-to-Methanol Conversion. *Angew. Chem., Int. Ed.* **2025**, *64*, No. e202416899.
(86) Redekop, E. A.; Cordero-Lanzac, T.; Salusso, D.; Pokle, A.; Oien-Odegaard, S.; Sunding, M. F.; Diplas, S.; Negri, C.; Borfecchia, E.; Bordiga, S.; Olsbye, U. Zn Redistribution and Volatility in $ZnZrO_x$ Catalysts for CO_2 Hydrogenation. *Chem. Mater.* **2023**, *35* (24), 10434−10445.
(87) Wang, J.; Liu, C.-Y.; Senftle, T. P.; Zhu, J.; Zhang, G.; Guo, X.; Song, C. Variation in the In_2O_3 Crystal Phase Alters Catalytic Performance toward the Reverse Water Gas Shift Reaction. *ACS Catal.* **2020**, *10* (5), 3264−3273.
(88) Dai, H.; Zhang, A.; Xiong, S.; Xiao, X.; Zhou, C.; Pan, Y. The Catalytic Performance of Ga_2O_3-CeO_2 Composite Oxides over Reverse Water Gas Shift Reaction. *ChemCatChem* **2022**, *14* (6), No. e202200049.
(89) Zhang, J.; Lu, S.; Su, X.; Fan, S.; Ma, Q.; Zhao, T. Selective formation of light olefins from CO_2 hydrogenation over Fe-Zn-K catalysts. *Journal of CO_2 Utilization* **2015**, *12*, 95−100.
(90) Tebar-Soler, C.; Martin-Diaconescu, V.; Simonelli, L.; Missyul, A.; Perez-Dieste, V.; Villar-Garcia, I. J.; Brubach, J. B.; Roy, P.; Haro, M. L.; Calvino, J. J.; Concepcion, P.; Corma, A. Low-oxidation-state Ru sites stabilized in carbon-doped RuO_2 with low-temperature CO_2 activation to yield methane. *Nat. Mater.* **2023**, *22* (6), 762−768.
(91) Tebar-Soler, C.; Diaconescu, V. M.; Simonelli, L.; Missyul, A.; Perez-Dieste, V.; Villar-Garcia, I.; Gomez, D.; Brubach, J. B.; Roy, P.; Corma, A.; Concepcion, P. Stabilization of the Active Ruthenium Oxycarbonate Phase for Low-Temperature CO_2 Methanation. *ACS Catal.* **2024**, *14* (6), 4290−4300.
(92) Yang, Q.; Fedorova, E. A.; Cao, D.-B.; Saraçi, E.; Kondratenko, V. A.; Kreyenschulte, C. R.; Lund, H.; Bartling, S.; Weiß, J.; Doronkin, D. E.; Grunwaldt, J.-D.; Brückner, A.; Jiao, H.; Kondratenko, E. V. Understanding Mn-modulated restructuring of Fe-based catalysts for controlling selectivity in CO_2 hydrogenation to olefins. *Nat. Catal.* **2025**, *8*, 595−606.
(93) Liu, W.; Yan, L.; Zhang, X.; Zhang, Z.; Dang, S.; Han, Y.-F.; Tu, W. Reactant-driven structural and chemical dynamics of Fe clusters for promoting hydrocarbon formation over a Na/FeZn catalyst. *J. Catal.* **2025**, *443*, 115940.
(94) Yu, W.; Zhu, M.; Yang, Z.; Han, Y.-F. Effects of Alumina Phases on the Structural Evolution of Iron Catalysts for the Catalytic Conversion of CO_2 to Olefins. *ACS Catal.* **2025**, *15* (4), 3428−3441.
(95) Fan, Q.; Liu, N.; Zhao, J.; Yu, Y.; Sun, Y.; Han, Y.; Zhang, J.; Wang, A.; Ge, Q.; Wei, J.; Sun, J. Regulating the location of metal promoters in CuFe-based catalysts for enhanced CO_2 hydrogenation to higher alcohols. *J. Energy Chem.* **2025**, *107*, 31−43.

https://doi.org/10.1021/jacsau.5c01671
JACS Au XXXX, XXX, XXX−XXX

(96) Ding, X.; Zhu, M.; Sun, B.; Yang, Z.; Han, Y.-F. An Overview on Dynamic Phase Transformation and Surface Reconstruction of Iron Catalysts for Catalytic Hydrogenation of CO_x for Hydrocarbons. *ACS Catal.* **2024**, *14* (8), 6137−6168.
(97) Zhu, J.; Wang, P.; Zhang, X.; Zhang, G.; Li, R.; Li, W.; Senftle, T. P.; Liu, W.; Wang, J.; Wang, Y.; Zhang, A.; Fu, Q.; Song, C.; Guo, X. Dynamic structural evolution of iron catalysts involving competitive oxidation and carburization during CO_2 hydrogenation. *Sci. Adv.* **2022**, *8* (5), No. eabm3629.
(98) Du, P.; Qi, R.; Zhang, Y.; Gu, Q.; Xu, X.; Tan, Y.; Liu, X.; Wang, A.; Zhu, B.; Yang, B.; Zhang, T. Single-atom-driven dynamic carburization over Pd_1-FeO_x catalyst boosting CO_2 conversion. *Chem.* **2022**, *8* (12), 3252−3262.
(99) Du, P.; Zhang, Y.; Qi, R.; Gu, Q.; Xu, X.; Wang, A.; Zhu, B.; Yang, B.; Zhang, T. Domino Effect of Catalysis: Coherence between Reaction Network and Catalyst Restructuring Accelerating Surface Carburization for CO_2 Hydrogenation. *J. Am. Chem. Soc.* **2025**, *147* (23), 19622−19631.
(100) Han, Y.; Fang, C.; Ji, X.; Wei, J.; Ge, Q.; Sun, J. Interfacing with Carbonaceous Potassium Promoters Boosts Catalytic CO_2 Hydrogenation of Iron. *ACS Catal.* **2020**, *10* (20), 12098−12108.
(101) Kim, K. Y.; Lee, H.; Noh, W. Y.; Shin, J.; Han, S. J.; Kim, S. K.; An, K.; Lee, J. S. Cobalt Ferrite Nanoparticles to Form a Catalytic Co-Fe Alloy Carbide Phase for Selective CO_2 Hydrogenation to Light Olefins. *ACS Catal.* **2020**, *10* (15), 8660−8671.
(102) Sun, X.; Yu, J.; Zada, H.; Han, Y.; Zhang, L.; Chen, H.; Yin, W.; Sun, J. Reaction-induced unsaturated Mo oxycarbides afford highly active CO_2 conversion catalysts. *Nat. Chem.* **2024**, *16*, 2044−2053.
(103) Liu, N.; Wei, J.; Xu, J.; Yu, Y.; Yu, J.; Han, Y.; Wang, K.; Orege, J. I.; Ge, Q.; Sun, J. Elucidating the structural evolution of highly efficient Co-Fe bimetallic catalysts for the hydrogenation of CO_2 into olefins. *Appl. Catal., B* **2023**, *328*, 122476.
(104) Han, J.; Han, Y.; Yu, J.; Sun, Y.; Cui, X.; Ge, Q.; Sun, J. Low-temperature CO_2 Hydrogenation to Olefins on Anorthic NaCoFe Alloy Carbides. *Angew. Chem., Int. Ed.* **2025**, *64* (9), No. e202420621.
(105) Tian, G.; Li, Z.; Zhang, C.; Liu, X.; Fan, X.; Shen, K.; Meng, H.; Wang, N.; Xiong, H.; Zhao, M.; Liang, X.; Luo, L.; Zhang, L.; Yan, B.; Chen, X.; Peng, H.-J.; Wei, F. Upgrading CO_2 to sustainable aromatics via perovskite-mediated tandem catalysis. *Nat. Commun.* **2024**, *15* (1), 3037.
(106) Cui, X.; Gao, P.; Li, S.; Yang, C.; Liu, Z.; Wang, H.; Zhong, L.; Sun, Y. Selective Production of Aromatics Directly from Carbon Dioxide Hydrogenation. *ACS Catal.* **2019**, *9* (5), 3866−3876.
(107) Hu, X.; Ding, C.; Chen, C.; Yang, Y.; Zhang, X.; Li, X.; Chen, B.; Wang, N. Mo-tailored CoFe alloy catalysts: Overcoming over-carburization via suppressing CO dissociation and tuning CH_x coupling for selective higher alcohol synthesis. *Appl. Catal., B* **2025**, *377*, 125515.
(108) Wang, M.; Wang, P.; Zhang, G.; Cheng, Z.; Zhang, M.; Liu, Y.; Li, R.; Zhu, J.; Wang, J.; Bian, K.; Liu, Y.; Ding, F.; Senftle, T. P.; Nie, X.; Fu, Q.; Song, C.; Guo, X. Stabilizing Co_2C with H_2O and K promoter for CO_2 hydrogenation to C_{2+} hydrocarbons. *Sci. Adv.* **2023**, *9* (24), No. eadg0167.
(109) Galhardo, T. S.; Braga, A. H.; Arpini, B. H.; Szanyi, J.; Gonçalves, R. V.; Zornio, B. F.; Miranda, C. R.; Rossi, L. M. Optimizing Active Sites for High CO Selectivity during CO_2 Hydrogenation over Supported Nickel Catalysts. *J. Am. Chem. Soc.* **2021**, *143* (11), 4268−4280.
(110) Du, X.; Li, R.; Xin, H.; Fan, Y.; Liu, C.; Feng, X.; Wang, j.; Dong, C.; Wang, C.; Li, D.; Fu, Q.; Bao, X. *In-Situ* Dynamic Carburization of Mo Oxide with Unprecedented High CO Formation Rate in Reverse Water-Gas Shift Reaction. *Angew. Chem., Int. Ed.* **2024**, *63* (51), No. e202411761.
(111) Zhao, B.; Sun, M.; Chen, F.; Shi, Y.; Yu, Y.; Li, X.; Zhang, B. Unveiling the Activity Origin of Iron Nitride as Catalytic Material for Efficient Hydrogenation of CO_2 to C_{2+} Hydrocarbons. *Angew. Chem., Int. Ed.* **2021**, *60* (9), 4496−4500.
(112) Zhang, Z.; Jia, L.; Guo, Y.; Li, Y.; Han, F.; Liao, B.; Dang, S.; Chen, F.; Tu, W.; Yu, X.; Han, Y.-F. N Restructuring of Iron-Based Catalysts Boosting the Formation of C_{2+} Olefins from CO_2 Hydrogenation. *ACS Catal.* **2025**, *15* (11), 8740−8752.
(113) Zhang, M.; Zhu, Y.; Yan, J.; Xie, J.; Yu, T.; Peng, M.; Zhao, J.; Xu, Y.; Li, A.; Jia, C.; He, L.; Wang, M.; Zhou, W.; Wang, R.; Jiang, H.; Shi, C.; Rodriguez, J.; Ma, D. A Highly Active Molybdenum Carbide Catalyst with Dynamic Carbon Flux for Reverse Water-Gas Shift Reaction. *Angew. Chem., Int. Ed.* **2025**, *64* (6), No. e202418645.
(114) Qi, Y.; Jiang, J.; Liang, X.; Ouyang, S.; Mi, W.; Ning, S.; Zhao, L.; Ye, J. Fabrication of Black In_2O_3 with Dense Oxygen Vacancy through Dual Functional Carbon Doping for Enhancing Photothermal CO_2 Hydrogenation. *Adv. Funct. Mater.* **2021**, *31* (22), 2100908.
(115) Kanuri, S.; Roy, S.; Chakraborty, C.; Datta, S. P.; Singh, S. A.; Dinda, S. An insight of CO_2 hydrogenation to methanol synthesis: Thermodynamics, catalysts, operating parameters, and reaction mechanism. *Int. J. Energy Research* **2022**, *46* (5), 5503−5522.
(116) Zhong, J.; Yang, X.; Wu, Z.; Liang, B.; Huang, Y.; Zhang, T. State of the art and perspectives in heterogeneous catalysis of CO_2 hydrogenation to methanol. *Chem. Soc. Rev.* **2020**, *49* (5), 1385−1413.

https://doi.org/10.1021/jacsau.5c01671
JACS Au XXXX, XXX, XXX−XXX